Supplementary Material of the manuscript "Functional Amyloids as Natural Storage of Peptide Hormones in Pituitary Secretory Granules"

Samir K. Maji[1†], Marilyn H. Perrin[2], Michael R. Sawaya[3], Sebastian Jessberger[4], Krishna Vadodaria[4], Robert A. Rissman[5], Praful S. Singru[6], K Peter R Nilsson[7], Rozalyn Simon[7], David Schubert[8], David Eisenberg[3], Jean Rivier[2], Paul Sawchenko[2], Wylie Vale[2] and Roland Riek[1,9*]

[1]Laboratory of Physical Chemistry, Eidgenössische Technische Hochschule, Wolfgang-Paulistrasse 10, CH-8093 Zürich

[2]The Clayton Foundation Laboratories for Peptide Biology, The Salk Institute for Biological Studies, 10010 North Torrey Pines Road, La Jolla, CA 92037

[3]Howard Hughes Medical Institute, UCLA-DOE Institute for Genomics and Proteomics, Box 951570, UCLA, Los Angeles CA, 90095-1570.

[4]Institute of Cell Biology, Department of Biology, ETH Zurich, 8093 Zürich, Switzerland

[5]Department of Neuroscience, University of California San Diego, 9500 Gilman Drive, La Jolla, CA, 92093-0662

[6]Division of Endocrinology, Diabetes and Metabolism, Tufts-Medical Center, Boston, MA, USA

[7] Department of Chemistry, IFM, Linköping University, SE-581 83 Linköping, Sweden

[8]Cellular Neurobiology Laboratory and [9]Structural Biology, The Salk Institute for Biological Studies, 10010 North Torrey Pines Road, La Jolla, CA 92037

†Present address; School of Bioscience and Bioengineering, IIT Bombay, Powai, Mumbai 400076, India

*Address for correspondence: roland.riek@phys.chem.ethz.ch

Peptide/Protein Hormones studied

The selected set of hormones include the main members of the peptide family of corticotropin releasing factor (CRF): human (rat) and ovine CRF, human and rat urocortin I (Ucn), mouse, rat and human Ucn II, human and mouse Ucn III and the related CRF-antagonist Sauvagine from frog skin (*1-4*), as well as the alpha-helical CRF (αCRF), designed to stabilize a helical fold by a lactam bridge (*5*). These hormone peptides from the hypothalamus are ~40 residues long and are of helical nature in solution (*6*). Hormone peptides chosen from the pancreas include the 29 residues-long human glucagon, glucagon-like peptide 1 and 2 (GLP-1 and GLP-2 (*7*)), and the 14-residues cyclic peptide hormone somatostatin comprising a β-turn-like structure in solution (*8*). Other glucagon-related peptides are GIP, exendin 4, secretin, helodermin, pituitary adenyl cyclase-activating polypeptides (PACAP-38), growth hormone releasing factor (GRF) and vasoactive intentinal polypeptide (VIP) (*7*). Pituitary hormones studied are the ~40 residues-long human, mouse (rat) and porcine adrenocorticotrophic hormones (ACTH) (*9*), ~30 residues-long human and ovine β-endorphin (*9*) as well as the 199-residue-long hormone protein human prolactin (*10*) composed of a complex helical bundle (*11*). A complete list of all the hormones including their amino acid sequence and location is given in Table S2.

Some Peptide and Protein Hormones Form Amyloid Fibrils *in vitro* in absence of heparin

Thio T is a fluorescent dye that binds to amyloid-like structures (*12*). Therefore, Thio T-binding studies provide qualitative information about the presence of amyloid fibrils. For the Thio T-binding studies all hormones were incubated at 37°C at a concentration of 2 mg/ml at granule-relevant pH 5.5 under slight agitation. The Thio T fluorescence was measured immediately after dissolution of all the peptides and after 30 days of incubation (Table S1, fig. S1). Among 40 hormones studied, 10 hormones showed significant Thio T binding after one month of incubation (fig. S1, Table S1). To further confirm the presence of amyloids, to formally determine the formation of amyloid fibrils by the hormone under study, and to characterize other possible assemblies present in the sample, electron microscopy (EM) was done on all hormones after 30 days of incubation at pH 5.5. Although amyloid fibrils might be

observed under the electron microscope even if only a minority of the sample forms fibrils, again only a subset of hormones shows fibril formation at day 30 (Table S1, fig. S2). It is noteworthy, that there is a perfect correlation between the Thio-T binding assay and the EM study. Finally, CD measurements were done to determine a possible structural transition towards a β-rich conformation during aggregation (*13*). The CD data suggest that after dissolution and preparation of monomeric hormones at day 0 of incubation, the hormones are either predominantly helical or unstructured in water (Table S1, fig. S3). However, upon incubation for 30 days, a conformational transition towards more β-sheet content was observed for all the peptides (with the exception of Neuromedin K) that show amyloid-like structure in the Thio T-binding assay and EM, as expected. In summary, about one quarter of peptide/protein hormones studied did undergo a structural transition into β-sheet-rich amyloid-like aggregates at pH 5.5.

11 out of 42 Peptide and Protein Hormones do not form Amyloid Fibrils *in vitro* in presence of heparin by all methods studied

In the study of amyloid fibril formation of hormones studied in presence of heparin most hormones form amyloid fibrils but nonconclusive data was obtained for neuromedin K, which appeared to form fibrils based on EM, Thio-T, CR and LCP binding without a conformational change in the CD. Similarly, salmon MSH and Oxytocin did not show a conformational change into β-sheet upon incubation, nor fibril formation under the EM, but bound Thio-T and LCP at low levels, suggesting a small amount of amyloid-like aggregates. Amongst the eight non amyloid-forming hormones: (i) The designed alpha-helical CRF serves as a negative control which can not aggregate because of a lactam bridge that stabilizes the helical monomeric fold, (ii) the human urocortin I (hUcn I) at pH 5.5 immediately precipitated upon solubilization, but formed a proto-fibrillar structure at non-physiological pH 8.5 (fig. S3) suggesting that its proper treatment and sample preparation are difficult.

X-ray Fiber Diffraction Indicates that Hormone Aggregates Comprise a Cross-β Sheet Structure

Amyloid fibrils comprise a cross β-sheet structure. In this structural entity the polypeptide chain is organized in β-sheets arranged parallel to the fibril axis with their constituent β-strands perpendicular to the fibril axis (*14, 15*). This conformation results in a simple diffraction pattern with ~4.7 Å meridional reflections from β-strand spacing and 7-12 Å equatorial reflections due to a spacing between β-sheets if there is an alignment of the fibrils (*15*). In absence of an alignment, the two reflections have a radial characteristic. To confirm the cross β-sheet structure of the hormone aggregates under study, x-ray diffraction experiments were performed for a few selected hormones listed in Table S1. All aggregates studied have the expected reflections around 4.7 Å (4.5-4.8 Å) and 10 Å (9.7 - 11.9 Å) (fig. S5D). In particular, the amyloid fibrils of human CRF in the absence of LMW heparin, of β-endorphin in the presence of LMW heparin, and VIP in the presence of LMW heparin have the reflections perpendicular to each other, whereas their absence in the other amyloid systems studied is attributed to a lack of sufficient alignment. Interestingly, the aggregates of Neuromedin K and AVP produced extra reflections at 4.4 Å suggesting unusual and cross β-sheet atypical properties.

Coaggregation of Hormones: ACTH with β-endorphin

The coagregation between ACTH into β-endorphin are discussed in the main text. More (indirect) support for the amyloid aggregation of ACTH into β-endorphin fibrils is based upon a comparative analysis of Thio T binding at different β-endorphin and ACTH concentrations. When β-endorphin fibrils are diluted by a factor of two with fresh buffer Thio T binding decreases by expected 50% (fig. S7). However, when β-endorphin fibrils were diluted by a factor of two with fresh buffer comprising ACTH monomer Thio T binding decreased only by 20%. Since monomeric ACTH does not bind Thio T, this experiment suggests coaggregation between β-endorphin and ACTH. Similar results were obtained when a mixture of monomeric ACTH and β-endorphin were incubated for two weeks (fig. S7).

Coaggregation of Hormones: ghrelin with obestatin

To further explore the possibility of a functional-relevant coaggregation of other hormones, the coaggregation behavior of ghrelin with obestatin was studied. Ghrelin and obestatin are derived from preproghrelin by post-translational processing and stored in the same secretory granules (*16*). Ghrelin does not aggregate *in vitro*, whereas obestatin does aggregate *in vitro,* either in the presence or absence of LMW heparin (Table S1). As shown in Figure S8 the ghrelin – obestatin mixture forms amyloid fibrils as measured by Thio T fluorescence and EM. Since the Thio T binding of the hormone mixture is almost doubled in intensity when compared to the obestatin-only experiment, a coaggregation of ghrelin with obestatin is indicated. To demonstrate directly that the amyloid fibrils are composed both of ghrelin and obestatin, 1D ^{1}H Nuclear Magnetic Resonance Spectroscopy (NMR) was performed with DMSO-solubilized amyloid aggregates harvested by high-speed centrifugation. The comparison between the 1D ^{1}H NMR spectra of the individual hormones in DMSO with the corresponding spectra from amyloids dissolved in DMSO suggests the presence of both hormones in the amyloid fibrils (fig. S8C). Since NMR is a quantitative method, the ratio between the two hormones present in the amyloid aggregates was determined to be 1:1.

Notably and as a control, no aggregation was observed in a mixture of ghrelin and ACTH, since both hormones are not able to aggregate individually and are not processed together. Additional examples of a possible coaggregation of hormones include the peptide component C-peptide that enhances the fibril formation of human amylin in β-cell secretory granules (*17*), and the exocrine protein amylase which does not aggregate by itself but co-aggregates with zymogen granule proteins in the regulated secretory pathway of exocrine cells (*18, 19*). Hence, the documented coaggregation of hormones that are processed and activated together in regulated secretory pathways suggests the presence of a highly-organized, specific, and structurally-controlled aggregation process that is functionally relevant.

Hormone Amyloids Release Active Monomer

The monomer release of hormone fibrils at pH 7.4 appears to be slightly faster than at pH 6 indicating that the aggregates are less stable at neutral pH. This effect was predicted by the

TANGO algorithm for a few of the hormones studied (fig. S6). This observation might be functionally relevant since granule-relevant hormone aggregates must be stable inside granules but release monomers upon secretion into the extracellular space at neutral pH.

Secretory Granules from the Rat Pituitary Comprise Amyloid-like Structures

To confirm observations from AtT20 cells *in vivo*, secretory granules were purified from adult rat pituitary following an established protocol using a 50% percoll gradient (see Material and Methods, Fig. S13). This procedure yielded two distinct layers of secretory granules termed light (L) and heavy (H) granules in line with previous studies (fig. S13) (*24*). Under the EM, the granules show the typical electron-dense core surrounded by membrane. The diameter of the granules is 100-400 nm. Tyr/Trp fluorescence measurements indicate the presence of protein/peptides in the purified granules. To determine that the purified granules from rat pituitary are amyloid-like in nature, Thio-T, Thio-S, and CR binding were measured by spectroscopy and microscopy. In addition, dot blot with fibril-specific antibody OC, CR birefringence and x-ray fiber diffraction were performed for the more abundant light-type secretory granules, where as for the heavy granules insufficient amounts could be purified for these studies (Fig. 3 and figs. S12C and S12D). The high binding of Thio-T, Thio-S and CR indicated the presence of an amyloid-like entity in the purified secretory granules. This observation is strengthened by the green-yellow birefringence of purified granules stained with CR which requires an ordered structure in the aggregates. Furthermore, the amyloid-specific antibody OC recognizes the purified secretory granules (Fig. 3G). The fiber diffraction pattern of purified light-type secretory granules shows a broad reflection at ~4.3 Å as well as a reflection at ~10 Å. Since the broad reflection at 4.3 Å might be a superposition of the membrane reflection at 4.1 Å and the inter-strand spacing of a b-sheet at 4.7 Å, the membranes of the granules were depleted by 1% Lubrol PX (pH 6). The EM in Fig. S13 illustrates that this treatment indeed reduced the presence of membrane significantly without disturbing the mesoscopic structure of the granules. The x-ray diffraction pattern with membrane-less granules of type light shows three reflections at 4.1 Å attributed to remaining membrane, at 4.7 Å interpreted as the spacing between strands in a β-sheet and a diffuse reflection at ~10 Å interpreted as the spacing between β-sheets (Note: the purified material is composed of a mixture of granules containing distinct hormones). The latter two reflections indicate the presence of a

cross-b-sheet structure typically observed in amyloid fibrils. The circular profiles for these reflections, rather than orthogonal positions for the two reflections, show that the amyloid-like entities in granules are not strongly aligned. In summary, these biophysical and biochemical studies strongly indicate that secretory granules purified from the rat pituitary comprise an amyloid-like structure of cross-β–sheet nature.

Material and Methods

Peptide synthesis. Peptides were synthesized using the solid phase approach and the Boc-strategy as reported earlier(*20*). Some peptides were also purchased from BACEM. The peptides were >98% pure by HPLC and capillary zone electrophoresis. The plasmid of human prolactin is a kind gift of Prof. PS Dannies and Prof. ME Hodsdon from Yale University School of Medicine. The hormone prolactin was expressed in *E. Coli* and purified following their previously published protocol (*21*). The identity of purified protein was tested by mass spectrometry. Dynamic light scattering and CD spectroscopy was used to make sure that the purified prolactin is in a monomeric well-folded helical state as expected from literature (*11*).

Hormone fibril formation. Initially, hormones were dissolved in 0.5 ml of 5% D-Mannitol (pH 5.5) and 0.01% sodium azide at a concentration of 2 mg/ml in 1.5 ml eppendorf tubes. The eppendorf tubes containing hormone solutions were placed into an EchoTherm model RT11 rotating mixture (Torrey Pines Scientific) with a speed corresponding 50 r.p.m. inside a 37°C incubator. Later, all the hormones were dissolved in 0.5 ml of 5% D-Mannitol (pH 5.5) and 0.01 % sodium azide at a concentration of 2 mg/ml in presence of 400 μM LMW heparin (5-kDa heparin from CalBioChem) in 1.5 ml eppendorf tubes and were incubated as described above. Similarly, mixed hormones samples were prepared as stated in the main text. In addition, several samples were prepared at pH 7.4, but otherwise identically. Prolactin was also prepared in presence of 400 μM chondroitin sulfate A instead of heparin. Toxicity

measurements were performed with samples that were prepared in absence of sodium azide. The fibril formation was monitored by EM, CD and time-resolved Thio T binding studies. Three independent experiments were performed for each sample.

Thioflavin T (Thio T) binding. A 10 μl aliquot of peptide sample was diluted to 500 μl 5% D-Mannitol containing 0.01% (w/v) sodium azide. The solution was mixed with 2 μl of 1 mM Thio T prepared in the same solution. Fluorescence was measured immediately after addition of Thio T. The experiment was measured on a spectrofluorimeter (Photon Technology International, Lawrenceville, NJ) with excitation at 450 nm and emission at 482 nm or between 460-500 nm. The fluorescence intensity at 482 nm was plotted in the graph. A rectangular 10 mm quartz micro-cuvette was used. Three independent experiments were performed for each sample.

Electron microscopy (EM). A 5 μl aliquot of peptide sample was diluted into 50 μl water to a peptide concentration of ~ 40 μM, spotted on a glow-discharged, carbon-coated Formvar grid (Electron Microscopy Sciences, Fort Washington, PA), incubated for 5 min, washed with distilled water, and then stained with 1% (w/v) aqueous uranyl formate solution. Uranyl formate solutions were filtered through 0.2 μm sterile syringe filters (Corning) before use. EM analysis was performed using a JEOL JEM-100CXII electron microscope at 80 kV with nominal magnifications between 36,000 and 72,000. Images were recorded digitally by using the SIS Megaview III imaging system. At least two independent experiments were carried out for each sample.

Congo Red (CR) birefringence. The Congo Red (CR) staining (*22*) was performed using the diagnostic amyloidal stain kit HT60 from Sigma. Briefly, samples were pelleted by centrifuge at 120,000 g and washed once by distilled water. Then, fibrils were placed in 100 μl of alkaline sodium chloride solution for 20 mins, with continuous vortexing. The continuous vortexing will enhance the uniform mixing of all fibril particles in solution. The mixture was then centrifuged briefly with 120,000 g and pellets were taken to stain with alkaline congo red

solution for 20 min with continuous vortexing. The mixtures were centrifuged briefly at 16000 g and pellets were washed twice with 500 μl of 20% ethanol. The pellets were resuspended in PBS and then spread evenly onto glass slides and air dried at room temperature. The slides were analyzed using a microscope equipped with two polarizer equipped with a CCD camera.

Trp and Tyr Fluorescence Spectroscopy. A 10 μl aliquot of hormone sample or purified granule sample were diluted to 500 μl 5% D-Mannitol containing 0.01% (w/v) sodium azide The fluorescence of Try and Trp was measured with excitation at 280 nm and emission at 300-500 nm. Typically, Tyr has an emission maximum ~ 305 nm and the Trp around 350 nm, respectively. The Trp signal is intrinsically much stronger than the Tyr one (*23*).

Secretory granule purification from AtT20 cells. AtT20 cells were grown in 10 cm dishes at 37°C, 5% CO2, 95% air for 5 days in Dulbecco's Modified Eagle's essential medium (GIBCO, Grand Island, NY) supplemented with 10% fetal calf serum. Isolation and purification of secretory granules from mouse anterior pituitary tumor cells (AtT20) were performed according to Carty et al (*24*) with slight modification. Briefly, the cells were collected at 90% confluence with HDB/0.5 mM EDTA, pelleted and washed by 1x HDB. The pellet was then resuspended in 0.25 M sucrose in 20 mM Tris-HCl buffer, 1 mM EDTA, pH 7.2 (SG buffer) at 23° C. The solution was homogenized with 10 strokes using a glass-Teflon homogenizer. The cellular homogenate was centrifuged for 5 min at 600 × g to pellet unbroken cells and nuclei (p_1) from the resultant supernatant (s_1). The pellet was washed with 25 ml of SG buffer and the resultant supernatant (S_2) was mixed with S_1 and centrifuged at 4000 g for 10 min which produced supernatant (S_3) and pellet (P_3). The supernatant was centrifuged 20 min at 22,000 × g. The crude granule pellet is rich in mitochondria, lysosomes, lightweight granules, and dense granules. It was resuspended in 2 ml of isolation medium and washed twice again by the same procedure. These two short washings at 23°C were reported to eliminate completely any tendency for subsequent cold-induced adhesiveness of the crude granule fraction. All subsequent steps were performed at 4°C. Next, the pellet was

resuspended in 400 μl SG buffer and homogenized. 200 μl of granules solutions were loaded on top of a preformed gradient composed of 9 ml of 50% Percoll (Sigma) solution in SG buffer. The preformed gradient was formed by centrifugation at 30,000 × g for 15 min (see also below for more details). The gradient formation was checked by Sigma density marker bead kit. After layering 200 μl of the resuspended crude granule fraction on top of the preformed gradient, centrifugation at 30,000 × g for 20 min was performed which, resulted in one distinct white band close to the top of the gradient. The upper band (Fraction 1, 2 ml) was removed by aspiration and centrifuged at 100,000 × g for 1 h. The pellet was diluted two fold with SG buffer and centrifuged 100,000 × g for 1h. This high-speed centrifugation step significantly reduced the Percoll content of the resulting fractions. The purified granules were stored at 4° C and used for all biophysical studies.

The isolated granules appear as dense structures, 200-500 nm, in diameter, round, oval, or polycyclic in shape, surrounded by a membrane usually separated from the granule core by a clear space. At high magnification, such a core reveals neither a crystalline nor a periodical organization. The fluorescence with excitation at 280 nm revealed an emission at 350 nm indicative of protein content (i.e. proteins with Trp residues). The immuno blot procedures further indicate that the purified materials are secretory granules.

Immunohistochemistry. Adult, male, wild type mice (C57BL/6) weighing 25-30 g were housed under standard environmental condition (light between 0600 and 1800 h, temperature 22 ± 1° C, chow and water *ad libitum*). Animals were anaesthetized with sodium pentobarbital and perfused transcardially with 10 ml phosphate buffered saline (PBS, 0.01 M, pH 7.4) followed by 50 ml 4% paraformaldehyde in phosphate buffer (0.1M, pH 7.4). The pituitary glands were dissected out and postfixed in the same fixative overnight at 4°C. The pituitary glands were cryoprotected in 25% sucrose solution in PBS overnight at 4°C, frozen in mounting media (Tissue-Tek, Torrance, CA) and sectioned on cryostat (CM 1850, Leica) at 12 μm thickness in coronal plane. Sections were mounted on Superfrost glass slides, air dried and stored at -20°C until processed further. The tissues were treated with hormone specific antibodies (1:10,000) and Thio S (1% w/v) or OC antibody (1:5000) for immunohistochemical studies. All protocols were approved by the Salk Institute's Institutional

Animal Care and Use Committee (IACUC). Images were acquired using a Leica SP1 confocal microscope equipped with a 40x objective (oil, NA 0.75-1.25). All imaging was done in sequential scan mode to exclude cross-bleeding between different channels. General contrast enhancements and color level adjustments were carried out using Adobe Photoshop CS3 for Mac

Monomer release from amyloid. Two 50 μl aliquots of 30 days-old hormone aggregates were harvested by centrifugation and "redissolved" in 50 μl of buffer each (5% D-mannitol) followed by dialysis through a 10 kDa cut-off membrane against 1 ml of buffer (10 mM Tris-HCl). A 50 kDa cut-off was used for prolactin since it has a molecular weight of ~20 kDa. For AVP (MW ~1 KDa) and Somatostatin (1.6 KDa) 3.5 kDa cut-off membranes were used. The cut-off was chosen to ensure that the released molecules are most likely monomeric. The Slide-A-Lyzer mini dialysis unit system was used (PIERCE, Rockford, IL, USA). Prior to transfer the fibril solution, the dialyisis units were soaked in 1 l of distilled water for 15 min for glycerol removal. The mini dialysis units were capped and placed into a 1-ml nunc cryo tube (Nunc, Denmark) containing 1ml of 10mM Tris-HCl, pH 6 and another cryo tube containing 1 ml of Tris-HCl, pH 7.4. Small magnetic bars were placed into individual tubes. The assembled units were placed onto a multicentered magnetic stirrer (Thermoeletric Corporation) under identical units. In the suitable interval the solution from inside the dialysis unit and outside the dialysis unit were taken for analysis. Care was taken to make sure that the membrane was exposed to solutions both in and outside and that any bubbles at the membrane interface were removed. The tubes were then incubated at room temperature. To measure the remaining amyloids inside the mini dialysis unit, a 3 μl aliquot was diluted into 150 μl 10 mM Tris-HCl, pH 7.4, 0.01% sodium azide, and Thio T was measured as described above. To determine the peptide concentration outside the membrane in the 1 ml cryo nunc tube, an aliquot of 150 μl of solution was taken from the releasing medium and fluorescence (excitation at 280 nm and emission in the range of 290–500 nm) and UV at 280 nm was measured. Following spectra recording, the released solution was returned and the dialysis system was reassembled as described above. Since human CRF does not contain any Tyr

or Trp, fluorescence measurements were replaced by CD measurements. At every suitable interval, the peptide solution (dialysate) was placed into a 0.5 cm path-length quartz cell (Hellma, Forest Hills, NY). Spectra were acquired using an instrument of JASCO 810 following procedure described above.

Tango Analysis. All peptide sequences were subjected to TANGO analysis, which predicts aggregation-prone regions in proteins and hormones. The algorithm is primarily based on simple physico-chemical principles of secondary structure formation and the assumption that aggregating sequence in proteins are fully buried (*25*). TANGO was performed at the two pHs 7 and 5 at 298 K at an ionic strength of 0.02, assuming a protein/peptide stability of -10. In addition, for the cyclic peptides disulfide bond formation was neglected and any possible side chain modifications were not considered.

Circular dichroism spectroscopy (CD). 10 μl of hormone solution was diluted in 5% D-mannitol to 200 μl. The peptide solution was placed into a 0.1 cm path-length quartz cell (Hellma, Forest Hills, NY). Spectra were acquired using a JASCO 810 instrument. All measurements were done at 23°C. Spectra were generally recorded over the wavelength range of 196-260 nm. Three independent experiments were performed with each sample. Raw data were manipulated by smoothing and subtraction of buffer spectra, according to the manufacturer's instructions.

Luminescent conjugated polymer binding.

The synthesis of the anionic LCP, p-FTAA, will be reported elsewhere (submitted). The LCP (*26*) was diluted to a final concentration of 15 μM in de-ionized water. 2 μl of each peptide sample was diluted into 96 μl of 2 M acetic acid/0.5 M NaCl, and 2 μl of the LCP stock solution was added to each sample and allowed to incubate at room temperature for 5 min. Excitation and emission spectra were recorded with a Tecan Saphire 2 plate reader. Excitation was at 450 nm and emission scans were recorded over the range of 480-700 with an emission bandwidth of 5 nm and ten repeated trials for each well.

Congo Red (CR) binding. A 5 μl aliquot of hormone sample was mixed with 80 μl of PBS buffer containing 10% ethanol. Then 15 μl of a 100 μM CR solution (filtered through 0.2 μM filter) in PBS containing 10% ethanol was added. After mixing, UV was measured from 300-700 nm. For the measurement of the CR-only spectrum, 15 μl of CR solution with 85 μl of PBS containing 10% ethanol was prepared. As a control, 5 μl aliquot of hormone mixed with 95 μl of PBS containing 10% ethanol was measured. Three independent experiments were performed for each sample.

Congo red fluorescence. A 2 μl aliquot of hormone sample was mixed with 198 μl of PBS containing 25 μM CR, pH 7.4. The CR containing buffer was filtered through 0.2μM syringe filter before the study. After 5 mins of incubation fluorescence was measured with excitation at 550 nm and emission of 570-650 nm. The experiment was measured on a spectrofluorimeter (Photon Technology International, Lawrenceville, NJ). A rectangular 10 mm quartz micro-cuvette was used. Three independent experiments were performed for each sample.

^{1}H NMR Spectroscopy. A lyophilized aliquot of hormone sample (~ 0.1 mg) was dissolved into 500 μl of dimethyl sulfoxide-d6 (d_6-DMSO) and 0.2% tri-fluor-acetic-acid (TFA). For the aggregated sample of gherlin - obestatin mixture, a 100 μl aliquot was centrifuged at high speed 120,000 ×g for 30 minutes and the pellet was dissolved into 500 μl of dimethyl sulfoxide-d6 (d_6-DMSO) and 0.2% TFA. 1D ^{1}H NMR spectra with an acquisition time of 0.3 s (4k points) were performed on an in house Bruker NMR spectrometer at 700 MHz ^{1}H frequency equipped with a triple resonance cryo-probe. Number of scans was 128 for the samples prepared from monomers, and 1k from the sample prepared from the pellet, respectively.

MTT assay. The 3-(4,5-dimethylthiazol-2-yl)-2,5-diphenyl tetrazolium bromide (MTT) assays were done in 96-well microtiter dishes containing 100 μl of medium per well. The CNS B12 cells (*27*) were used for the study. The B12 cells were plated in a medium containing 5%

dialyzed sera, and the day after plating, the test reagents were added. After 20 h, 10 μl of a 5 mg/ml MTT stock in PBS was added per well, and the incubation continued for 4 hours. Finally, 100 μl of a solution containing 50% dimethylformamide and 20% SDS (pH 4.8) was added. The next day, absorption values at 570 nm were determined with an automatic microtiter plate reader.

Neuronal survival assay. E18 rat hippocampal neurons were dissociated with trypsin and plated at 3×10^6 per 35 mm poly-lysine coated tissue culture dishes in neurobasal medium (GIBCO, grand Isaland, NY) containing B27 supplements without antioxidants (GIBCO). The cells were cultured for 14 days and the test compounds were added. These include 30 days aged hCRF and Aβ(1-42) fibrils at the indicated concentrations. The control solvent containing 5% D-mannitol also was diluted as with the fibrils. Cell viability was assayed 2 days later using fluorescent live/dead stain (Molecular Probes). Ten fields of 20-30 cells each and in the control dishes were counted.

X-ray diffraction. Hormones were incubated in aggregation buffer for 30 days. The completion of fibril formation was confirmed by CD and Thio T and EM. The fibrils solution were centrifuged using Beckman Coulter Airfuge, Air-Driven ultracentrifuge with 22 PSI (126,000 g) for 1 hr. Pelleted samples were washed in water to prevent the formation of salt crystals that might otherwise grow from residual buffer components during the sample drying process. Salt crystals are undesirable as they produce interfering diffraction patterns. Specifically, the pellets were suspended in 100 μL of water, and then re-pelleted in an Eppendorf Centrifuge 5417C with fixed angle rotor (F-45-30-11) at 13000 rpm for 10 min. The washed pellets were resuspended in 5 μl of water and pipette between two fire-polished glass rods and left to dry for 2-3 days. Ideally, the dried sample would stretch between glass rods creating a fiber-like projection that could be placed in the X-ray beam to produce a diffraction pattern. However, the sample most frequently formed only a thin coat over the glass rod. The coat was scraped from the glass rod since the coat is much thinner than the diameter of the x-ray beam, and glass produces a shadow in the path of the X-ray beam. The

coat was then mounted on a MiTeGen MicroMesh (catalog number M3-L11-10), nearly transparent to X-rays. 50% polyethylene glycol 4000 (PEG4000) was used to fix the film to the micromesh. PEG4000 produces little background pattern (diffuse 3.5 Å ring) compared to ten other cryo-protectant molecules tested. The dried material was placed in an X-ray beam at 100 K for a 5 min exposure. A rotating anode generator (Rigaku FR-E) and imaging plate detector (RaxisIV++) were used for the data collection.

Immuno fluorescence study of cells. The AtT20 cells were plated on poly-L-lysine coated coverslips in 10% FBS/DMEM (~$2x10^5$ cells/coverslip). After 24 hours, coverslips were washed with PBS (3X) and the cells were fixed by 4% PFA for 1hr at RT. Fixed cells were washed with PBS (3X) and subsequently blocked in 5% Donkey serum (DS), 0.01% Triton in PBS for 1 hr at RT. The cells were then incubated with antibodies to ACTH (anti mouse, a-ACTH (1-24)(AB-1) (1:2000), Oncogene) and β-endorphin (anti-rabbit, AB5028, 1:2000) in 5% Donkey serum (DS), 0.01% Triton in PBS for 24 h, 4°C. Cells were washed 3x, 10 min with PBS and then incubated with Cy3-conjugated donkey anti mouse IgG and goat anti-rabbit AlexaFluor 488 (each 1:600, Jackson ImmunoResearch, West Grove, PA) in PBS, 5% DS, 1% triton, 60 min, RT. The coverslips were washed 3X with PBS and mount. For imaging we used the Leica TCS SP2 A0BS confocal microscope.

CRF Receptor activation (cAMP assay).

Chinese hamster ovary cells stably expressing the type 1 CRF receptor were grown to confluence in DMEM, 10% FBS, and then trypsinized and replated into 12-well COSTAR plates; the cells were allowed to recover for 24 hr. The medium was changed to 0.1% BSA/DMEM at least 2 h before treatment. The cells were preincubated for 30 min with 0.1 mM 3-isobutyl-1-methylxanthine and then exposed to fibrils or CRF (as control) for 20 min at 37°C. Intracellular cAMP was extracted and measured from triplicate wells using a radioimmunoassay kit (Biomedical Technologies).

Membrane-less granule preparation of Secretory granules from Rat pituitary and AtT20 cells. In 1 ml of secretory granule suspension (20 mM Tris-HCl, 0.25 M sucrose, 1 mM EDTA, pH 7.2) 100 μL of 10% Lubrol (Sigma) was added at 4°C. Once the entire solution became more transparent a few μl of 1 mM HCl was added to adjust the suspension to an acidic pH of 6 to make sure that the membrane-less granules do not dissolve readily. The granules were incubated for 45 min on ice and then centrifuged at 120,000 × g. The white, membrane-less granules were found at the bottom of the eppendorf tube, stored at 4° C, and successively used for the structural studies.

Secretoy granule purification from rat pituitary. Isolation and purification of dense granules from intact rat pituitary glands were performed according to Carty et al. (*24*) with slight modification. Briefly, rat pituitary were dissected from 6-8 weeks old, male Sprague Dawley rats (housed with a constant 12h light/dark cycle and food ad libitum; Janvier). After removal of the fibrous capsule, 15-17 pituitaries were minced and homogenized in an isolation medium of 0.25 M sucrose in 20 mM Tris-HCl buffer, 1mM EDTA, pH 7.2 at 23°C. The cellular homogenate was centrifuged for 5 min at 600 × g to pellet unbroken cells and nuclei and the resultant supernatant was centrifuged 20 min at 9700 × g. The crude granule pellet obtained was then resuspended in 2 ml of isolation medium and washed twice again by the same procedure. These two short washings at 23°C were reported to eliminate completely any tendency for subsequent cold-induced adhesiveness of the crude granule fraction. All subsequent steps were performed at 4°C. Dense granules were purified from other subcellular organelles by centrifugation through an isotonic preformed density gradient of 50% Percoll, 0.25 M sucrose in 20mM Tris-HCl, 1 mM EDTA, pH 7.2. Percoll is a high density, low viscosity, biologically inert suspension of minute silica beads, contributing less than 7 mosm to the gradient solution. Continuous s-shaped gradients were preformed by centrifugation of 10 ml of Percoll gradient solution for 15 min at 30,000 × g in a standard preparative centrifuge. After 2.0 ml of the resuspended crude granule fraction was layered a top the preformed gradient, centrifugation at 30,000 × g for 20 min resulted in two distinct bands separated by over three-fourths of the gradient. The upper band (Fraction 1, A, 2 ml),

containing mitochondria, lysosomes, and lightweight granules, was removed by aspiration, as was the clear middle fraction (Fraction 2, 5 ml). The lower band, containing the dense granules (Fraction 3, 3 ml, C), was recovered and the granules were washed once in ice-cold isolation medium. The fractions were diluted two fold by isolation buffer and centrifuged 100,000 × g for 1h and repeated this process two times. This high-speed centrifuge significantly reduced the percoll content of the resulting fractions. The purified granules were kept at 4°C and used for all biophysical studies. All protocols were approved by the Salk Institute's Institutional Animal Care and Use Committee (IACUC).

Supplementary Figure Captions

Figure S1. Thio T binding of hormones studied are indicative of amyloid fibril formation. Thio T fluorescence of hormones are shown which were incubated for 0 days (black), 30 days (red) at 37°C at a concentration of 2 mg/ml in 5% D-mannitol (pH 5.5) under slight agitation. In addition, Thio T fluorescence of hormones are shown which were incubated for 14 days (blue) at 37° C at a concentration of 2 mg/ml in 5% D-mannitol (pH 5.5) with 0.4 mM LMW heparin under slight agitation. For human prolactin, aggregation was studied in presence of chondroitin sulfate A instead of LMW heparin as indicated. All hormones are labeled in accordance to Tables S1 and S2. The intensity of Thio T fluorescence is shown as arbitrary units (AU). The error bars represent the standard deviation of three independent experiments.

Figure S2. Morphologies of hormones under study incubated for 30 days in absence of LMW heparin. The aggregations of the hormones were followed at 37° C at a concentration of 2 mg/ml in 5% D-mannitol (pH 5.5) under slight agitation. The aggregation of human Urocortin I was studied at pH 8.5 because of low solubility at pH 5.5. Transmission electron microscopy (TEM) of negative stained samples was performed. Scale bars are 500 nm.

Figure S3. Morphologies of 42 hormones incubated for 30 days in presence of LMW heparin are indicative of amyloid fibril formation. The aggregations of the hormones were followed at 37° C at a concentration of 2 mg/ml in the presence of 0.4 mM LMW heparin in 5% D-mannitol (pH 5.5) under slight agitation. The human prolactin (hPRL) was fibrillized in presence of 400 µM chondroitin sulfate A. Transmission electron microscopy (TEM) of negative stained samples was performed. Scale bars are 500 nm.

Figure S4. Aggregation-induced conformational change of the hormones under study into β-sheet rich aggregates revealed by circular dichroism (CD). CD spectra of hormones are

shown which were incubated for 0 days in absence of LMW heparin (black), 30 days in absence of heparin (red), and 14 days in presence of LMW heparin (blue) at conditions described in figure captions S1 and S2.

Figure S5. (A-B) Congo-Red (CR), (C) LCP (p-FTAA) binding and x-ray fiber diffraction (D) of hormones studied are indicative of amyloid fibril formation. (A-B) CR binding can be measured by the "red shift" change of its absorption maximum from 490 nm as indicated by the black bar at 490 nm, or/and by an increase of the dye's molar absorptivity. The blue spectrum labeled with "mannitol" is the control. (C) LCP fluorescence of hormones is shown. The samples for both measurements were incubated for 14 days at 37° C at a concentration of 2 mg/ml in 5% D-mannitol (pH 5.5) with 0.4 mM LMW heparin under slight agitation. (D) X-ray fiber diffraction of a selected set of hormone amyloid fibrils. hCRF, hUcnII and hUcnIII are fibrillized in 5% D-mannitol at 37°C with slight agitation, where as GRF-40, VIP, GIP, pNPY, Neuro K, hβ-end, and AVP are fibrillized in presence of 0.4 mM LMW heparin. Human prolactin (hPRL) is fibrillized in presence of chondroitin sulfate A. The two reflections at ~4.7 Å and ~10 Å consistent with a cross-β-sheet structure are labeled.

Figure S6. Aggregation-prone segments of the hormones studied predicted by the TANGO algorithm at pH 5 (red) and pH 7 (black) as indicated. Values > 0 are indicative of aggregation-prone segments along the amino acid sequence.

Figure S7. Coaggregation of ACTH with β-endorphin. (A) Thio T binding between various mixtures of ACTH and with β-endorphin. Thio T binding was measured for 14 days-old ACTH (1 mg/ml), 14 days-old β-endorphin both at concentrations of 2 mg/ml and 1 mg/ml (1/2 diluted), 14 days-old mixture of ACTH – β-endorphin with 1 mg/ml hormone concentration each (total hormone concentration was 2 mg/ml). 14 days-old β-endorphin (2 mg/ml) with fresh addition of freshly prepared 2 mg/ml ACTH solution resulting in a 1 mg/ml hormone concentration each. The hormones were incubated under slight agitation at 37° C in the

presence of 0.4 mM LMW heparin in 5% Dmannitol (pH 5.5). The observed increase in Thio T binding upon addition or in the presence of ACTH indicates coaggregation of ACTH and β-endorphin. (B) Colocalization of the two hormones in the tumor cell line AtT20 by double immunohistochemistry with mouse ACTH (red) and rabbit endorphin antibodies (green). The nuclear marker DAPI shown in blue.

Figure S8. Coaggregation peptide hormones. Coaggregation of ghrelin with obestatin measured by (A) EM, (B) Thio T binding, and (C) ^{1}H-NMR. (D) Failed coaggregation between CRF and ACTH by Trp fluorescence and (E) Thio T binding. (A) EM of ghrelin (2 mg/ml), obestatin (2 mg/ml) and ghrelin – obestatin mixture (1mg/ml concentration of each hormone) at 37° C at in presence of 0.4 mM LMW heparin in 5% D-mannitol (pH 5.5) incubated under slight agitation for 14 days. Both obestatin and the ghrelin – obestatin mixture form amyloid fibrils, whereas ghrelin-only is unable to form fibrils. Scale bars are 200 nm. (B) Thio T binding was measured for 14 days-old ghrelin (2 mg/ml), 14 days-old obestatin (2 mg/ml), and 14 days-old mixture of ghrelin – obestatin with 1 mg/ml hormone concentration each. The hormones were incubated under slight agitation at 37°C in presence of 0.4 mM LMW heparin in 5% D-mannitol (pH 5.5). The observed increase in Thio T binding upon addition or in presence of ghrelin indicates coaggregation of ghrelin and obestatin (see also main text). (C) ^{1}H-NMR spectroscopy was measured for the in DMSO-dissolved pellet of an aggregated sample of the ghrelin – obestatin mixture (black). For reference, the individual hormones were also dissolved in DMSO: ghrelin (red), obestatin (blue). The data reveal that both ghrelin and obestatin are present in the aggregates formed in a ratio of 1:1. (D) Trp fluorescence spectroscopy was measured for an aggregated sample of ACTH – CRF mixture. Since CRF lacks a Trp residue, the fluorescence measurement reveals the presence of ACTH. The absence of a significant Trp signal in the pellet of the ACTH-CRF mixture upon high speed centrifugation (displayed in black) and the presence of the Trp signal in the supernatant thereof (displayed in blue) indicates that ACTH does not

coaggregate with CRF. Furthermore, a fresh solution of a mixture of ACTH – CRF (m) displayed in blue and a fresh solution of ACTH (m) displayed in red were measured accordingly. (E) Thio T binding was measured for 14 days-old mixture (1:1) of ACTH (2 mg/ml) and CRF (2 mg/ml), 14 days-old CRF (2 mg/ml), the pellet of the ACTH-CRF mixture upon high speed centrifugation (CRF-ACTH-hep (p)) and the supernatant thereof (CRF-ACTH-hep(s)). The hormones were incubated under slight agitation at 37° C in presence of 0.4 mM LMW heparin in 5% D-mannitol (pH 5.5). The observed decrease in Thio T binding of ACTH-CRF mixture compared to CRF only indicates ACTH slightly inhibits the amyloid formation by CRF. The Thio T binding of ACTH-CRF and pelleted ACTH-CRF are similar indicates fibrils contain only CRF.

Figure S9. Monomer release profiles of amyloid fibrils of β-endorphin (A), 1:1 mixture of ACTH-β-endorphin (B), AVP (C), Somatostatin (D) and hPRL (E). Hormones were incubated for 14 days in presence of 0.4 mM LMW heparin to form fibrils. hPRL was fibrilized in presence of 0.4mM chondroitin sulfate A. The amyloid formation was checked by Thio T binding and EM. 50μL of the fibrils were centrifuged at 120,000 g. The corresponding pellets were redissolved and dialyzed against 10 mM Tris-HCl buffer (pH 7.4). At regular intervals, Thio T binding was performed to measure fibril content inside the dialysis membrane shown in blue and labeled by the left y-axis. The peptide/protein content in the released medium was measured by UV shown in red and labeled by the right y-axis. The units of Thio T fluorescence and UV are arbitrary (AU).

Figure S10. Toxicity measurements of hormone aggregates. (A) MTT reduction by the CNS cell line B12 in the presence of hormone samples (20 μM) were measured with respect to buffer alone (5% D-mannitol (pH 5.5), 400 μM of heparin). Aβ(1-40) and Aβ(1-42) samples were included as positive controls. The hormones and Aβ's used were incubated under slight agitation for 14 days at 37°C at peptide/protein concentrations of 2 mg/ml in presence of 0.4 mM LMW heparin in 5% D-mannitol (pH 5.5). (B) and (C) the survival of rat primary neurons were measured after 2 days in the presence of amyloid fibrils of human CRF and Aβ(1-42)

amyloid fibrils. (B) Fluorescence microscopy of viable cells labeled with the fluorescence dye Calcein (Molecular Porbes). (C) Cell viability quantified to buffer control ($p < 0.01$ for CRF at 10 and 20 μM and for Aβ(1-42) at all concentrations, respectively).

Figure S11. Characterization of secretory granules purified from the AtT20 cell line. (A) Purification of secretory granules by percoll gradient centrifugation (see Material and Method). On the left is shown the Sigma density marker bead kit. On the right, the band of the secretory granules is indicated by an arrow. (B) Negative-stained EM image of secretory granules. In the blow up, secretory granules are shown without (top) and with membrane depletion (bottom). The arrow indicates the membrane. Scale bars are 500 nm. (C) Trp and Tyr fluorescence spectroscopy of secretory granules indicating the presence of peptide/proteins in the purified preparations. (D) The dot blot study with ACTH antibody suggests that the purified secretory granules contain ACTH as expected. As positive control, the dot blot of synthetic human ACTH is shown, too.

Figure S12. CR binding and CR fluorescence of purified secretory granules from (A,B) the AtT20 cell line and (C,D) heavy (H, blue) and light (L, black) secretory granules from rat pituitary are indicative of the presence of amyloids. (A,C) CR fluorescence between 570-650 is shown of purified secretory granules (black and blue) and buffer-only (red). (B, D) Similarly, CR absorbance between 400 and 600 nm is presented to show the “red shift” change of its absorption maximum from 490 nm, which is a signature for amyloids (black and blue). The buffer-only measurement is shown in red.

Figure S13. Characterization of secretory granules purified from rat pituitary. (A) Purification of secretory granules by percoll gradient centrifugation. On the left is shown the Sigma density marker bead kit. On the right, the light (L) and heavy (H) secretory granules are indicated. (B) Trp and Tyr fluorescence spectra of both light (in black) and heavy (in blue) secretory granules indicating the presence of peptide/proteins in the purified preparations. (C) The dot blot study with ACTH and β-endorphin antibodies suggests that (in contrast to

heavy secretory granules; data not shown) the light secretory granules contain ACTH and β-endorphin as expected (*28*). As a control, dot blots against synthetic ACTH and β-endorphin is shown also as indicated. (D) Negative-stained EM images of light and heavy secretory granules. The apparent membrane around the granules is indicated by an arrow. In addition, the EM of membrane-less light secretory granules is also shown.

Figure S14. Cartoon of secretory granule formation. The formation of secretory granules is shown with the hypothesis that hormones aggregate (selectively) into amyloids upon prohormone processing (indicated by a scissor). The membrane recruiting around the aggregates for the granule maturation happens spontaneously because of the inherent nature of amyloids to interact with membrane. Upon secretion monomeric functional hormone is released from the amyloid aggregate for activity. The amyloid conformation of the hormone is highlighted by arrows indicative of β-sheet structure. The functional conformation of the hormone is highlighted by a helix. The cell compartments are labeled.

Supplementary References.

1. W. Vale, J. Spiess, C. Rivier, J. Rivier, *Science* **213**, 1394 (1981).
2. J. Spiess, J. Rivier, C. Rivier, W. Vale, *Proc. Natl. Acad. Sci. U. S. A.* **78**, 6517 (1981).
3. K. Lewis *et al.*, *Proc. Natl. Acad. Sci. U. S. A.* **98**, 7570 (2001).
4. T. M. Reyes *et al.*, *Proc. Natl. Acad. Sci. U. S. A.* **98**, 2843 (2001).
5. J. Rivier *et al.*, *J. Med. Chem.* **41**, 2614 (1998).
6. C. R. Grace *et al.*, *J. Am. Chem. Soc.* **129**, 16102 (2007).
7. T. J. Kieffer, J. F. Habener, *Endocr. Rev.* **20**, 876 (1999).
8. C. R. Grace *et al.*, *J. Med. Chem.* **46**, 5606 (2003).
9. T. L. O'Donohue, D. M. Dorsa, *Peptides* **3**, 353 (1982).
10. H. Friesen, P. Hwang, *Annu. Rev. Med.* **24**, 251 (1973).
11. C. Keeler, P. S. Dannies, M. E. Hodsdon, *J. Mol. Biol*. **328**, 1105 (2003).
12. H. LeVine, *Methods Enzymol.* **309**, 274 (1999).
13. D. M. Walsh *et al.*, *J. Biol. Chem.* **274**, 25945 (1999).
14. M. Sunde, C. Blake, *Adv. Protein. Chem.* **50**, 123 (1997).
15. M. Sunde *et al.*, *J. Mol. Biol.* **273**, 729 (1997).
16. M. Gronberg, A. V. Tsolakis, L. Magnusson, E. T. Janson, J. Saras, *J. Histochem. Cytochem.* **56**, 793 (2008).
17. P. Westermark, Z. C. Li, G. T. Westermark, A. Leckstrom, D. F. Steiner, *FEBS Lett.* **379**, 203 (1996).
18. V. Colomer, K. Lal, T. C. Hoops, M. J. Rindler, *EMBO J.* **13**, 3711 (1994).
19. S. U. Gorr, S. Y. Tseng, *Biochem. Biophys. Res. Commun.* **215**, 82 (1995).
20. G. Jiang *et al.*, *J. Med. Chem.* **44**, 453 (2001).
21. B. J. Sankoorikal, Y. L. Zhu, M. E. Hodsdon, E. Lolis, P. S. Dannies, *Endocrinology* **143**, 1302 (2002).

22. W. E. Klunk, R. F. Jacob, R. P. Mason, *Anal. Biochem.* **266**, 66 (1999).

23. J. R. Lakowicz, *Principles of fluorescence spectroscopy* (Kluwer Academic/Plenum Publishers, New York, ed. 2nd, 1999), pp. 698.

24. S. E. Carty, R. G. Johnson, A. Scarpa, *J. Biol. Chem.* **257**, 7269 (1982).

25. A. M. Fernandez-Escamilla, F. Rousseau, J. Schymkowitz, L. Serrano, *Nat. Biotechnol.* **22**, 1302 (2004).

26. C. J. Sigurdson *et al.*, *Nat. Methods* **4**, 1023 (2007).

27. D. Schubert *et al.*, *Nature* **249**, 224 (1974).

28. A. Costoff, W. H. McShan, *J. Cell. Biol.* **43**, 564 (1969).

Table S1: Biochemical and biophysical properties of aggregates of hormones

No	NAME	D0-CD^{M}(¶)	D30-CD^{M}(¶)	D15-CD^{h}	ThT^{m}	ThT^{h}	EM^{M}	EM^{h}	CR^{h}	LCP1^{h}	X-ray^{h}	Amyloid^{M}	Amyloid^{h}
1	r/hCRF	helix	β-sheet	β-sheet	+	+	fib	fib	+	+	+	+	+
2	oCRF	helix+RC	β-sheet	β-sheet	+	+	fib	fib	+	+	ND	+	+
3	hUcn	helix	helix	helix	+	+	nfib‡	nfib‡	-	-	ND	-	-
4	rUcn	helix	β-sheet	β-sheet	+	+	fib	fib	+	+	ND	+	+
5	hUcnII	helix	helix	β-sheet	-	+	nfib	fib	+	+	+	-	+
6	mUcnII	helix+RC	helix+RC	β-sheet	-	+	nfib	fib	+	+	ND	-	+
7	rUcnII	helix+RC	helix+β	β-sheet	-	+	nfib	fib	+	+	ND	-	+
8	hUcnIII	helix	β-sheet	β-sheet	+	+	fib	fib	+	+	+	+	+
9	mUcnIII	helix	β-sheet	β-sheet	+	+	fib	fib	+	+	ND	+	+
10	Sauv	helix+RC	β-sheet	β-sheet	+	+	fib	fib	+	+	ND	+	+
11	sfUro	helix	β-sheet	β-sheet	+	+	fib	fib	+	+	ND	+	+
12	hGhrelin	RC	RC	RC	-	-	nfib	nfib	-	-	ND	-	-
13	hGRF-40	RC	RC	β-sheet	-	+	nfib	fib	+	+	+	-	+
14	hGRF44	RC	RC	β-sheet	-	+	nfib	fib	+	+	ND	-	+
15	VIP	RC	RC	β-sheet	-	+	nfib	fib	+	+	+	-	+
16	sCalcitonin	RC	RC	β-sheet	-	+	nfib	fib	+	+	ND	-	+
17	Glucagon	RC+helix	β-sheet	β-sheet	+	+	fib	fib	+	+	ND	+	+
18	GLP-1	RC+helix	β-sheet	β-sheet	+	+	fib	fib	+	+	ND	+	+
19	GLP-2	helix	β-sheet	β-sheet	+	+	fib	fib	+	+	ND	+	+
20	Secretin	helix	helix	β-sheet	-	-	nfib	nfib	-	-	ND	-	-
21	GIP	helix	β-sheet	β-sheet	+	+	fib	fib	+	+	+	+	+
22	Exendin4	helix	Helix	β-sheet	-	+	nfib	fib	-	+	ND	-	+
23	Helodermin	helix	Helix	β-sheet	-	+	nfib	fib	+	+	ND	-	+
24	pGalanin	RC	RC	β-sheet	-	+	nfib	fib	+	+	ND	-	+
25	hGalanin	RC	RC	β-sheet	-	+	nfib	fib	+	ND	ND	-	+
26	cPACAP	RC	RC	β-sheet	-	+	nfib	fib	+	+	ND	-	+
27	Neuro K	helix	helix	helix	+	+	fib	fib	-	+	+	-	+
28	Obestatin	RC	β-sheet	β-sheet	+	+	fib	fib	+	ND	ND	+	+
29	Bombesin	RC	RC	β-sheet	-	+	nfib	fib	+	+	ND	-	+
30	pNPY	helix	helix	β-sheet	-	+	nfib	fib	+	+	ND	-	+
31	GRP	RC	RC	β-sheet	-	+	nfib	fib	+	+	ND	-	+
32	hACTH	RC	RC	RC	-	-	nfib	nfib	-	-	ND	-	-
33	rACTH	RC	RC	RC	-	-	nfib	nfib	-	-	ND	-	-
34	pACTH	RC	RC	RC	-	-	nfib	nfib	-	-	ND	-	-
35	hβ-endorphin	RC	RC	β-sheet	-	+	nfib	fib	+	+	+	-	+
36	oβ-endorphin	RC	RC	β-sheet	-	+	nfib	fib	+	ND	ND	-	+
37	Salmon MSH	turn	turn	turn	-	+	nfib	nfib	-	-	ND	-	+
38	Oxytocin	turn	turn	turn	-	+	nfib	nfib#	-	+	ND	-	+
39	AVP	Turn+RC	Turn+RC	β-sheet	-	+	nfib	Fib	+	+	+	-	+
40	Somatostatin	RC	RC	β-sheet	-	+	nfib	fib	+	+	ND	-	+
41	hPRL	helix	helix	helix*	-	+	nfib	fib	+	ND	+	-	+
42	α-CRF	helix	helix	helix	-	-	nfib	nfib	-	-	ND	-	-

CD^{m},CD in 5% D-mannitol; ThT^{m}, ThT binding in 5% Mannitol; EM^{m}, EM in 5% Mannitol; CD^{h}, CD in presence of heparin; ThT^{h}, ThT binding in presence of heparin, EM^{h}, EM in presence of heparin; Fib, fibrils; nfib, no fibrils; ND, not determined

‡Protofibrillar structure observed

#Globular structure which bind ThT dye

*hPRL was studied in 1:1 CHS A

¶Visual observation of secondary structure by CD

Table S2: Hormones studied

No	NAME	Amino acid SEQUENCE	ABUNDANCE/isolated	MW	AA
1	r/h CRF	SEEPPISLDL TFHLLREVLE MARAEQLAQQ AHSNRKLMEI I	Hypothalamus	4758	41
2	oCRF	SQEPPISLDL TFHLLREVLE MTKADQLAQQ AHSNRKLLDI A	Hypothalamus	4671	41
3	hUcn	DNPSLSIDLT FHLLRTLLEL ARTQSQRERA EQNRIIFDSV	Hypothalamus	4697	40
4	rUcn	DDPPLSIDLT FHLLRTLLEL ARTQSQRERA EQNRIIFDSV	Hypothalamus	4708	40
5	hUcnII	IVLSLDVPIG LLQILLEQAR ARAAREQATT NARILARV	Hypothalamus	4154	38
6	mUcnII	VILSLDVPIG LLRILLEQAR YKAARNQAAT NAQILAHV	Hypothalamus	4154	38
7	rUcnII	VILSLDVPIG LLRILLEQAR NKAARNQAAT NAQILARV	Hypothalamus	4124	38
8	hUcnIII	FTLSLDVPTN IMNLLFNIAK AKNLRAQAAA NAHLMAQI	Hypothalamus	4138	38
9	mUcnIII	FTLSLDVPTN IMNILFNIDK AKNLRAKAAA NAQLMAQI	Hypothalamus	4173	38
10	Sauvagine	EGPPISIDLS LELLRKMIEI EKQEKEKQQA ANNRLLLDTI	Frog skin	4618	40
11	Sf Urotensin	NDDPPISIDL TFHLLRNMIE MARIENEREQ AGLNRKYLDEV	Fish Hypothalamus	4871	41
12	hGhrelin	GSSFLSPEHQ RVQQRKESKK PPAKLQPR	Stomach	3371	28
13	hGRF-40	YADAIFTNSY RKVLGQLSAR KLLQDIMSRQ QGESNQERGA	Hypothalamus	4544	40
14	hGRF-44	YADAIFTNSY RKVLGQLSAR KLLQDIMSRQ QGESNQERGA RARL	Hypothalamus	5040	44
15	VIP	HSDAVFTDNY TRLRKQMAVK KYLNSILN	Hypothalamus, pituitary	3327	28
16	sCalcitonin	CSNLSTCVLG KLSQELHKLQ TYPRTNTGSG TP	Thyroid	3435	32
17	Glucagon	HSQGTFTSDY SKYLDSRRAQ DFVQWLMNT	Pancreas	3482	29
18	GLP-1	HDEFERHAEG TFTSDVSSYL EGQAAKEFIA WLVKGRG	Pancreas	4170	37
19	GLP-2	HADGSFSDEM NTILDNLAAR DFINWLIQTK ITD	Pancreas	3766	33
20	Secretin	HSDGTFTSEL SRLREGARLQ RLLQGLV	Duodenum	3039	27
21	GIP	YAEGTFISDY SIAMDKIHQQ DFVNWLLAQK GKKNDWKHNI TQ	GI tract	4983	42
22	Exendin4	HGEGTFTSDL SKQMEEEAVR LFIEWLKNGG PSSGAPPPS	Salivary gland of the lizard	4186	39
23	Helodermin	HSDAIFTQQY SKLLAKLALQ KYLASILGSR TSPPP	Venom of Gila monster (heloderma suspectum)	3844	35
24	pGalanin	GWTLNSAGYL LGPHAIDNHR SFHDKYGLA	Colon and pituitary	3211	29
25	hGalanin	GWTLNSAGYL LGPHAVGNHR SFSDKNGLTS	Colon and pituitary	3157	30
26	cPACAP	HSDGIFTDSY SRYRKQMAVK KYLAAVLGKR YKQRVKNK	Hypothalamus	4536	38
27	Neuromedin K	DMHDFFVGLM	Porcine spinal cord	1210	10
28	Obestatin	FNAPFDVGIKLSGVQYQQHS	Stomach	2549	23
29	Bombesin	QRLGNQWAVG HLM	Frog skin	1600	13
30	pNPY	YPSKPDNPGE DAPAEDLARY YSALRHYINL ITRQRY	Porcine hypothalamus	4254	36
31	GRP	VPLPAGGGTV LTKMYPRGNH WAVGHLM	Post-ganglionic fibres of the vagus nerve	2859	27
32	hACTH	SYSMEHFRWG KPVGKKRRPV KVYPNGAEDE SAEAFPLEF	Pituitary	4541	39
33	pACTH		Pituitary		39
34	m/rACTH	SYSMEHFRWG KPVGKKRRPV KVYPNVAENE SAEAFPLEF	Pituitary	4582	39
35	hβ-endorphin	YGGFMTSEKS QTPLVTLFKN AIIKNAYKKG E	Pituitary	3465	31
36	oβ-endorphin	YGGFMTSEKS QTPLVTLFKN AIVKNAHKKG Q	Pituitary	3424	31
37	Salmon MSH	SYSMEHFRWG KPVG	Pituitary	1680	14
38	Oxytocin	CYIQNCPLG (disulfide bond)	Pituitary	1007	9
39	ArgVasopressin	CYFQNCPRG (disulfide bond)	Pituitary	1084	9
40	Somatostatin-14	AGCKNFFWKT FTSC (disulfide bond)	Pancreas	1639	14
41	hPRL	LPICPGGAAR CQVTLRDLFD RAVVLSHYIH NLSSEMFSEF DKRYTHGRGF ITKAINSCHT SSLATPEDKE QAQQMNQKDF LSLIVSILRS WNEPLYHLVT EVRGMQEAPE AILSKAVEIE EQTKRLLEGM ELIVSQVHPE TKENEIYPVW SGLPSLQMAD EESRLSAYYN LLHCLRRDSH KIDNYLKLLK CRIIHNNNC	Pituitary	22898	199
42	αCRF(30-33)	PPISLDLTFN LLREVLEIAK AEQEAEEAAK NRLLLEA	agonist		

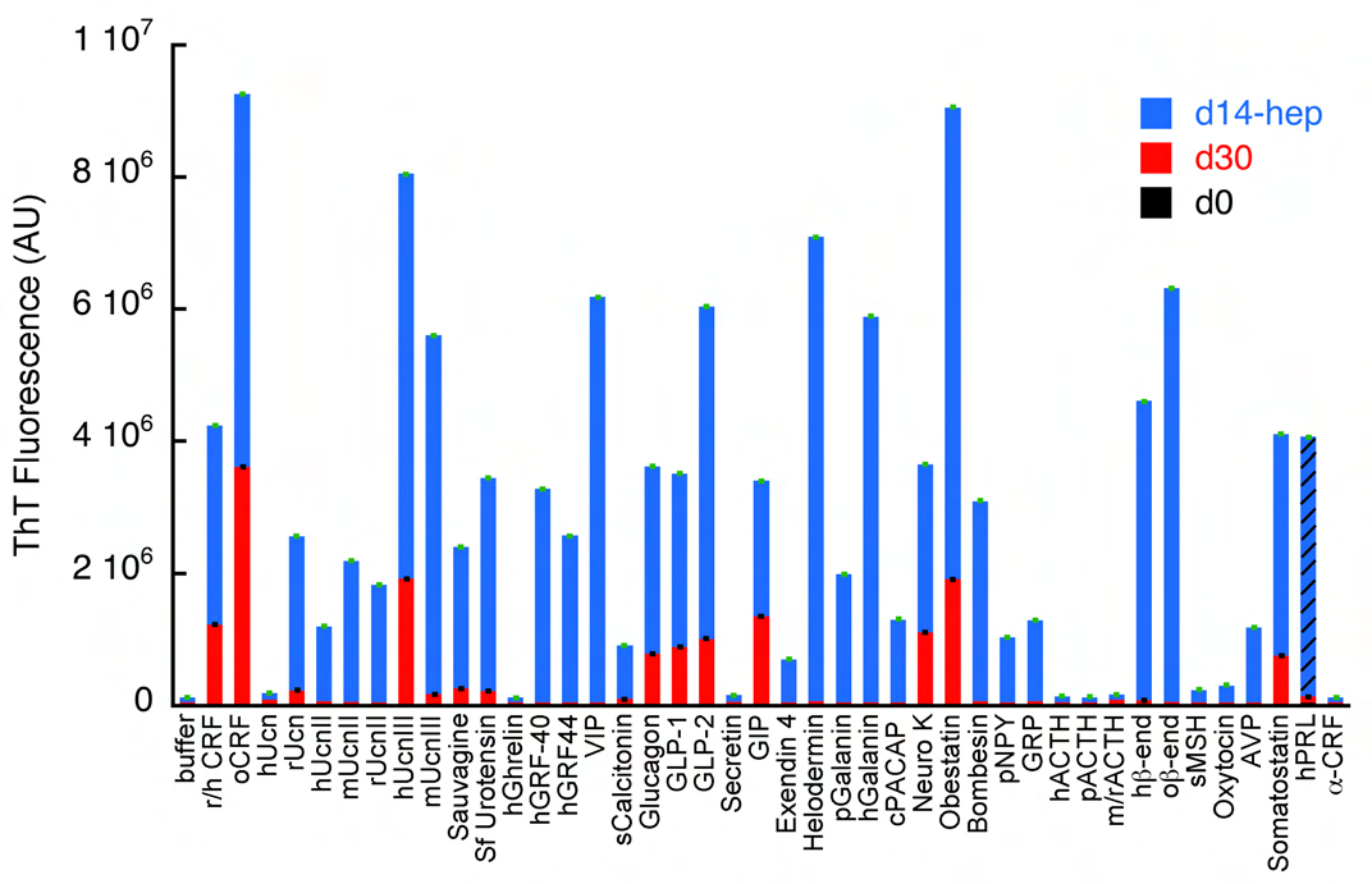
ThT Fluorescence (AU)
1 10^7
8 10^6
6 10^6
4 10^6
2 10^6
0
d14-hep
d30
d0
buffer
r/h CRF
oCRF
hUcn
rUcn
hUcnII
mUcnII
rUcnII
hUcnIII
mUcnIII
Sauvagine
Sf Urotensin
hGhrelin
hGRF-40
hGRF44
VIP
sCalcitonin
Glucagon
GLP-1
GLP-2
Secretin
GIP
Exendin 4
Helodermin
pGalanin
hGalanin
cPACAP
Neuro K
Obestatin
Bombesin
pNPY
GRP
hACTH
pACTH
m/rACTH
hβ-end
oβ-end
sMSH
Oxytocin
AVP
Somatostatin
hPRL
α-CRF

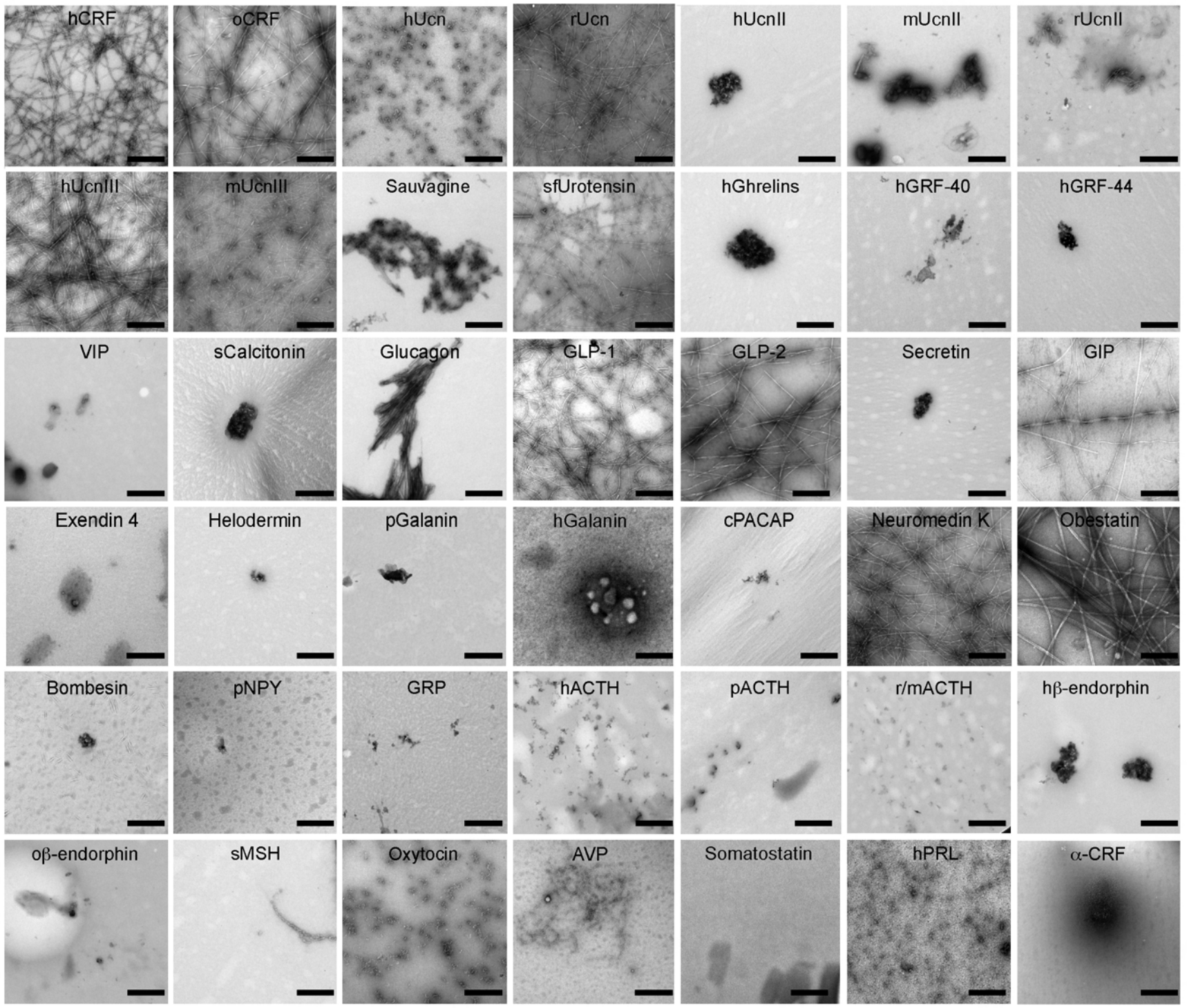
hCRF
oCRF
hUcn
rUcn
hUcnII
mUcnII
rUcnII
hUcnIII
mUcnIII
Sauvagine
sfUrotensin
hGhrelins
hGRF-40
hGRF-44
VIP
sCalcitonin
Glucagon
GLP-1
GLP-2
Secretin
GIP
Exendin 4
Helodermin
pGalanin
hGalanin
cPACAP
Neuromedin K
Obestatin
Bombesin
pNPY
GRP
hACTH
pACTH
r/mACTH
hβ-endorphin
oβ-endorphin
sMSH
Oxytocin
AVP
Somatostatin
hPRL
α-CRF

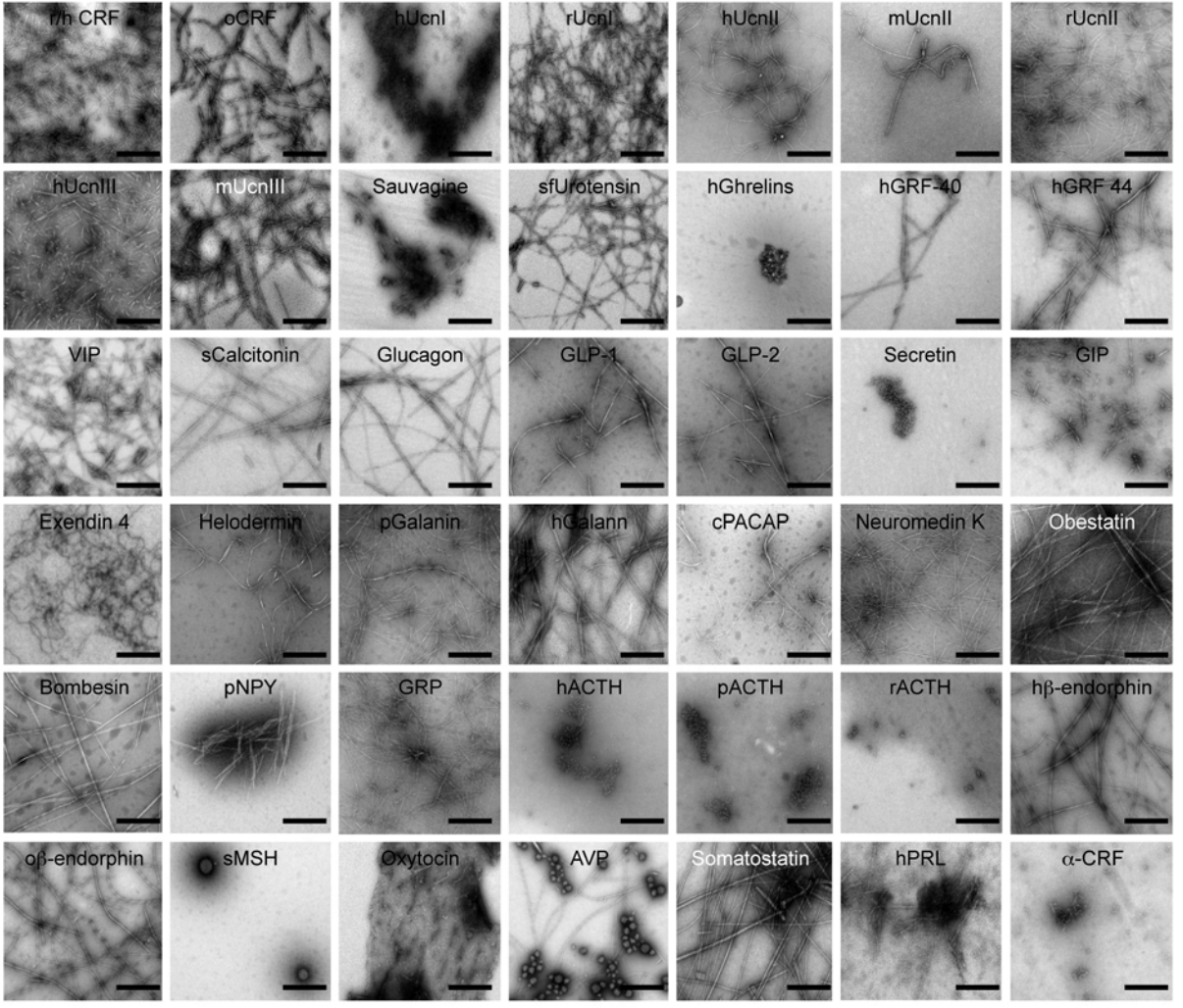
r/h CRF
oCRF
hUcnI
rUcnI
hUcnII
mUcnII
rUcnII
hUcnIII
mUcnIII
Sauvagine
sfUrotensin
hGhrelins
hGRF-40
hGRF 44
VIP
sCalcitonin
Glucagon
GLP-1
GLP-2
Secretin
GIP
Exendin 4
Helodermin
pGalanin
hGalann
cPACAP
Neuromedin K
Obestatin
Bombesin
pNPY
GRP
hACTH
pACTH
rACTH
hβ-endorphin
oβ-endorphin
sMSH
Oxytocin
AVP
Somatostatin
hPRL
α-CRF

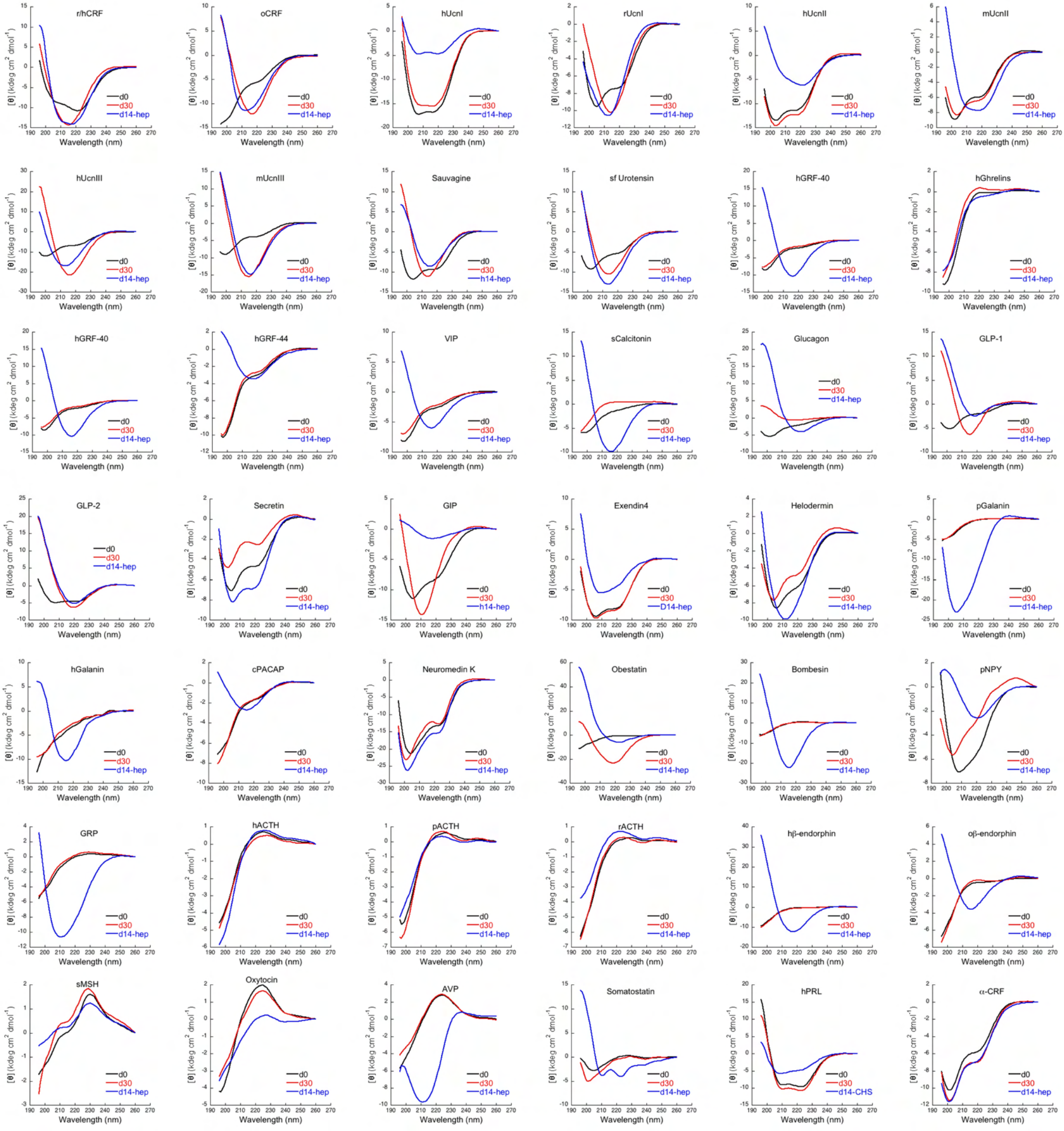
r/hCRF
oCRF
hUcnI
rUcnI
hUcnII
mUcnII
hUcnIII
mUcnIII
Sauvagine
sf Urotensin
hGRF-40
hGhrelins
hGRF-40
hGRF-44
VIP
sCalcitonin
Glucagon
GLP-1
GLP-2
Secretin
GIP
Exendin4
Helodermin
pGalanin
hGalanin
cPACAP
Neuromedin K
Obestatin
Bombesin
pNPY
GRP
hACTH
pACTH
rACTH
hβ-endorphin
oβ-endorphin
sMSH
Oxytocin
AVP
Somatostatin
hPRL
α-CRF
[θ] (kdeg cm2 dmol-1)
Wavelength (nm)
d0
d30
d14-hep
h14-hep
D14-hep
d14-CHS

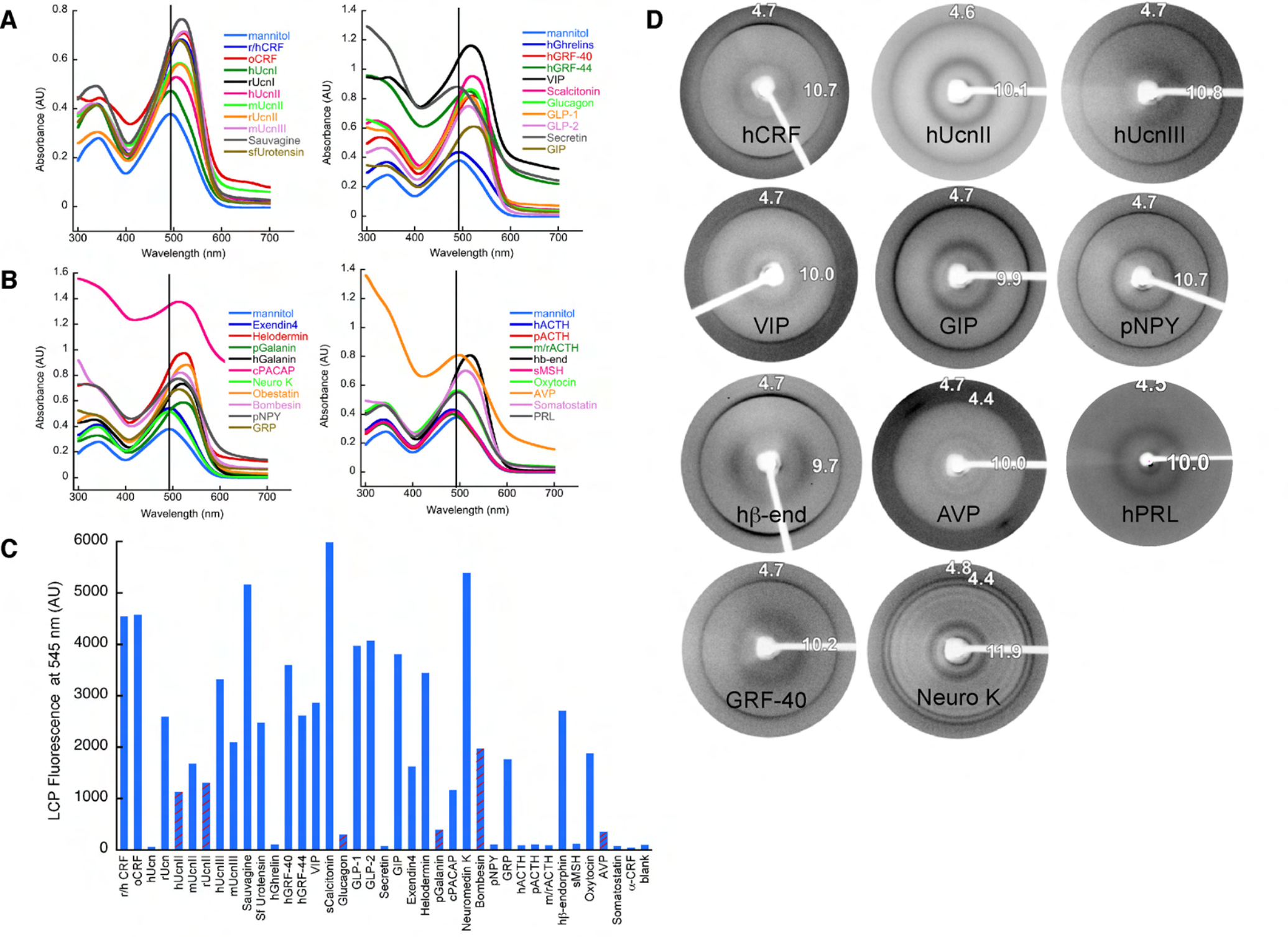
A
Absorbance (AU)
Wavelength (nm)
mannitol
r/hCRF
oCRF
hUcnI
rUcnI
hUcnII
mUcnII
rUcnII
mUcnIII
Sauvagine
sfUrotensin
mannitol
hGhrelins
hGRF-40
hGRF-44
VIP
Scalcitonin
Glucagon
GLP-1
GLP-2
Secretin
GIP
B
Absorbance (AU)
Wavelength (nm)
mannitol
Exendin4
Helodermin
pGalanin
hGalanin
cPACAP
Neuro K
Obestatin
Bombesin
pNPY
GRP
mannitol
hACTH
pACTH
m/rACTH
hb-end
sMSH
Oxytocin
AVP
Somatostatin
PRL
C
LCP Fluorescence at 545 nm (AU)
r/h CRF
oCRF
hUcn
rUcn
hUcnII
mUcnII
rUcnII
hUcnIII
mUcnIII
Sauvagine
Sf Urotensin
hGhrelin
hGRF-40
hGRF-44
VIP
sCalcitonin
Glucagon
GLP-1
GLP-2
Secretin
GIP
Exendin4
Helodermin
pGalanin
cPACAP
Neuromedin K
Bombesin
pNPY
GRP
hACTH
pACTH
m/rACTH
hβ-endorphin
sMSH
Oxytocin
AVP
Somatostatin
α-CRF
blank
D
hCRF
hUcnII
hUcnIII
VIP
GIP
pNPY
hβ-end
AVP
hPRL
GRF-40
Neuro K

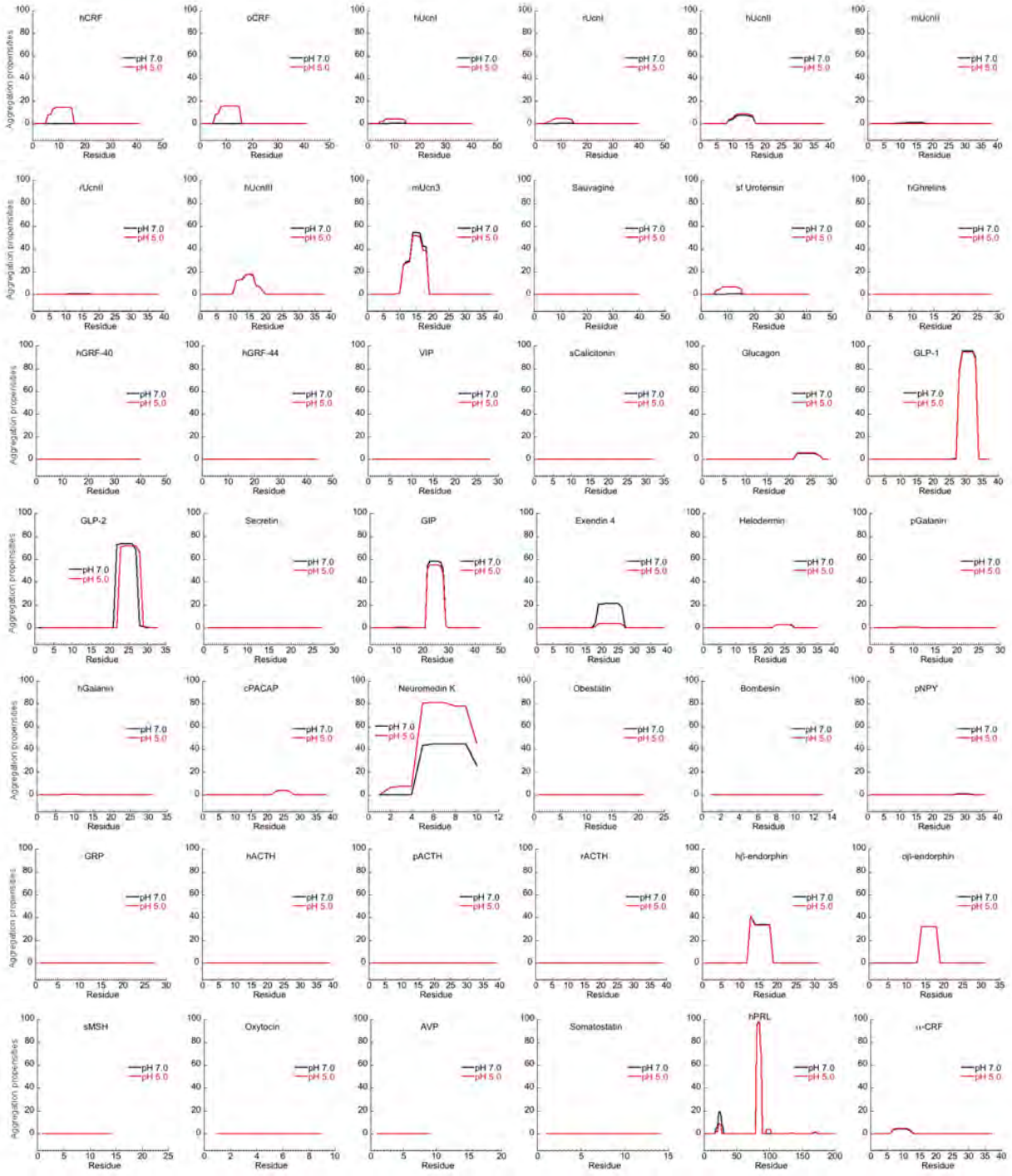
hCRF
oCRF
hUcnI
rUcnI
hUcnII
mUcnII
rUcnII
hUcnIII
mUcn3
Sauvagine
sf Urotensin
hGhrelins
hGRF-40
hGRF-44
VIP
sCalicitonin
Glucagon
GLP-1
GLP-2
Secretin
GIP
Exendin 4
Helodermin
pGalanin
hGalanin
cPACAP
Neuromedin K
Obestatin
Bombesin
pNPY
GRP
hACTH
pACTH
rACTH
h(i-endorphin
o(i-endorphin
sMSH
Oxytocin
AVP
Somatostatin
hPRL
rr-CRF
pH 7.0
pH 5.0
Residue
Aggregation propensities

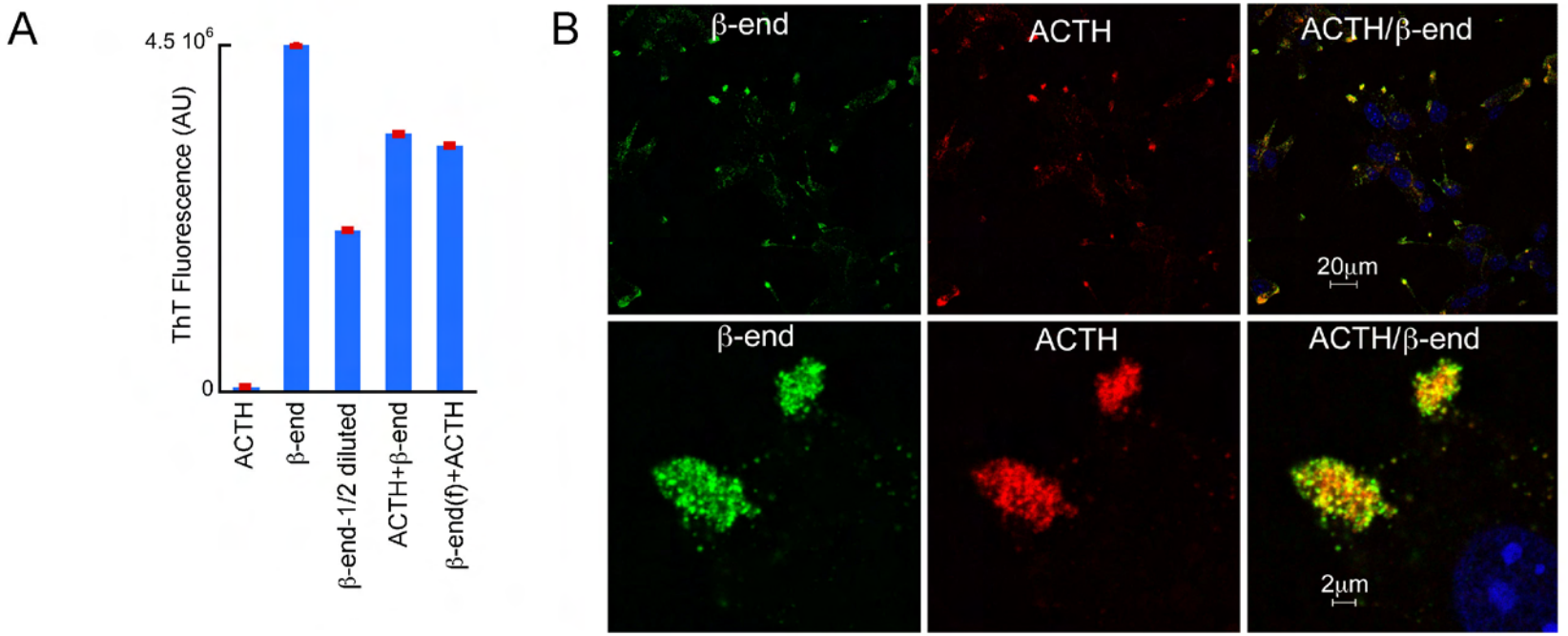
A
4.5 10^6
ThT Fluorescence (AU)
0
ACTH
β-end
β-end-1/2 diluted
ACTH+β-end
β-end(f)+ACTH
B
β-end
ACTH
ACTH/β-end
20μm
β-end
ACTH
ACTH/β-end
2μm

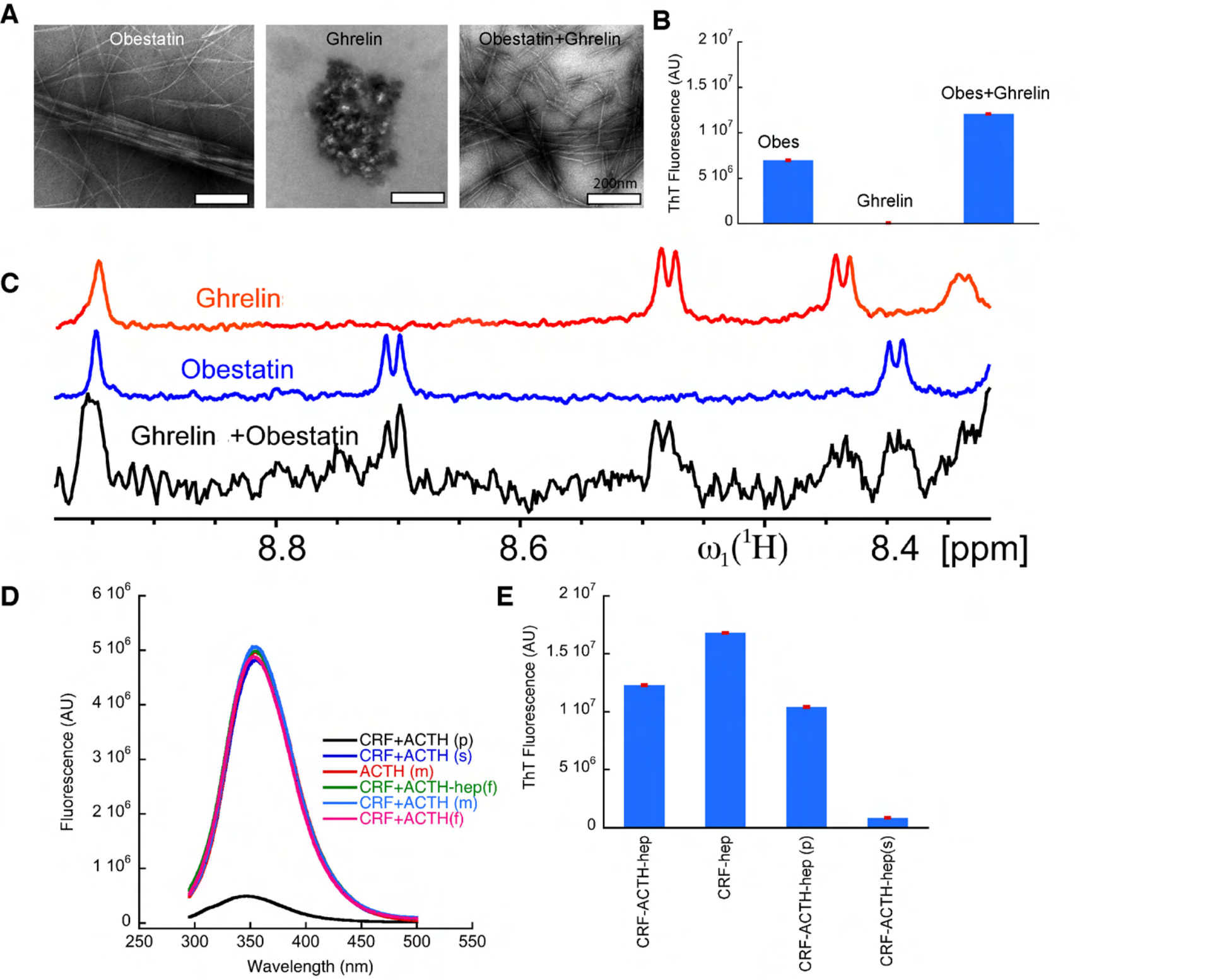
A
Obestatin
Ghrelin
Obestatin+Ghrelin
200nm
B
ThT Fluorescence (AU)
2 10^7
1.5 10^7
1 10^7
5 10^6
0
Obes
Ghrelin
Obes+Ghrelin
C
Ghrelin
Obestatin
Ghrelin +Obestatin
8.8
8.6
ω1(1H)
8.4
[ppm]
D
Fluorescence (AU)
6 10^6
5 10^6
4 10^6
3 10^6
2 10^6
1 10^6
0
250
300
350
400
450
500
550
Wavelength (nm)
CRF+ACTH (p)
CRF+ACTH (s)
ACTH (m)
CRF+ACTH-hep(f)
CRF+ACTH (m)
CRF+ACTH(f)
E
ThT Fluorescence (AU)
2 10^7
1.5 10^7
1 10^7
5 10^6
0
CRF-ACTH-hep
CRF-hep
CRF-ACTH-hep (p)
CRF-ACTH-hep(s)

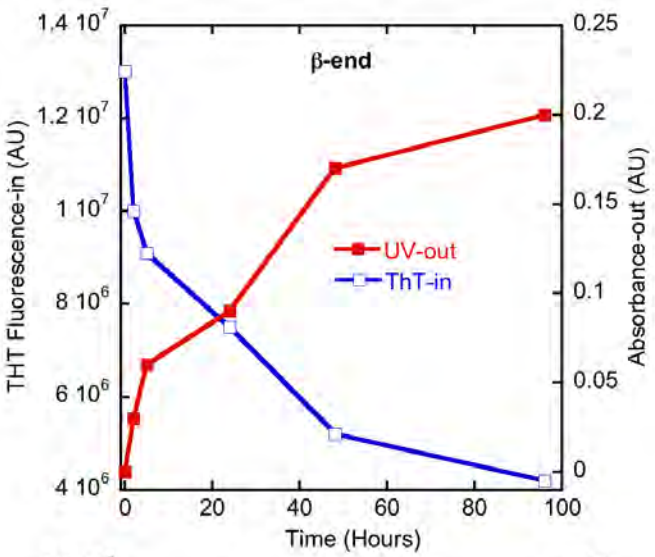
β-end
UV-out
ThT-in
THT Fluorescence-in (AU)
Absorbance-out (AU)
Time (Hours)
1.4 10^7
1.2 10^7
1 10^7
8 10^6
6 10^6
4 10^6
0.25
0.2
0.15
0.1
0.05
0
0
20
40
60
80
100

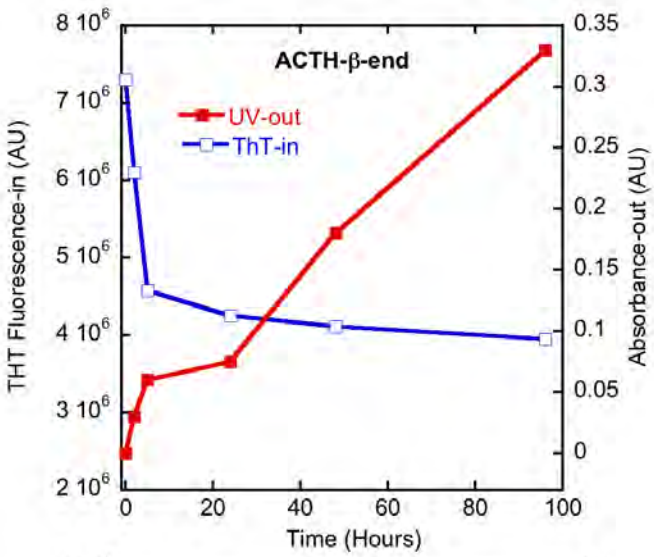
ACTH-β-end
UV-out
ThT-in
THT Fluorescence-in (AU)
Absorbance-out (AU)
Time (Hours)
8 10^6
7 10^6
6 10^6
5 10^6
4 10^6
3 10^6
2 10^6
0.35
0.3
0.25
0.2
0.15
0.1
0.05
0
0
20
40
60
80
100

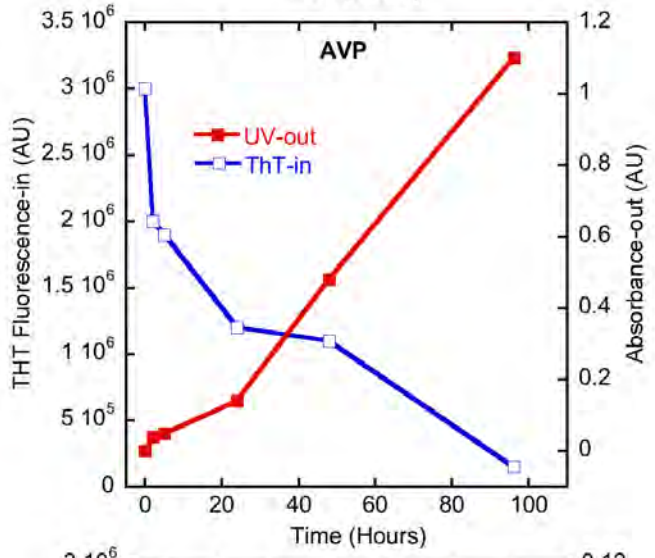
AVP
UV-out
ThT-in
THT Fluorescence-in (AU)
Absorbance-out (AU)
Time (Hours)
3.5 10^6
3 10^6
2.5 10^6
2 10^6
1.5 10^6
1 10^6
5 10^5
0
1.2
1
0.8
0.6
0.4
0.2
0
0
20
40
60
80
100

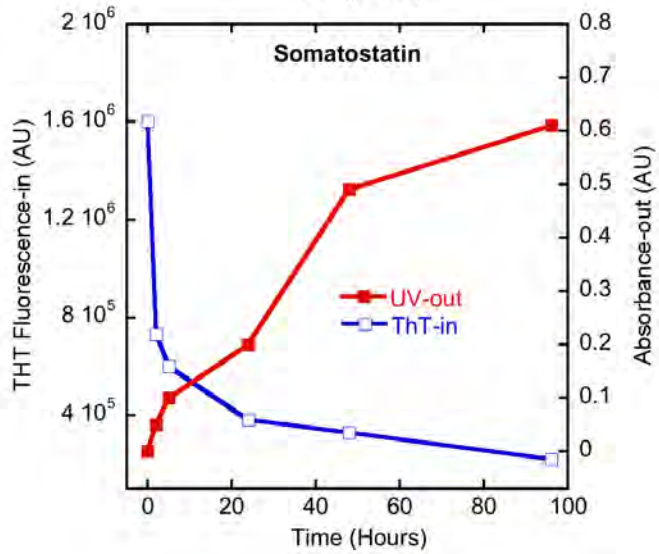
Somatostatin
UV-out
ThT-in
THT Fluorescence-in (AU)
Absorbance-out (AU)
Time (Hours)
2 10^6
1.6 10^6
1.2 10^6
8 10^5
4 10^5
0.8
0.7
0.6
0.5
0.4
0.3
0.2
0.1
0
0
20
40
60
80
100

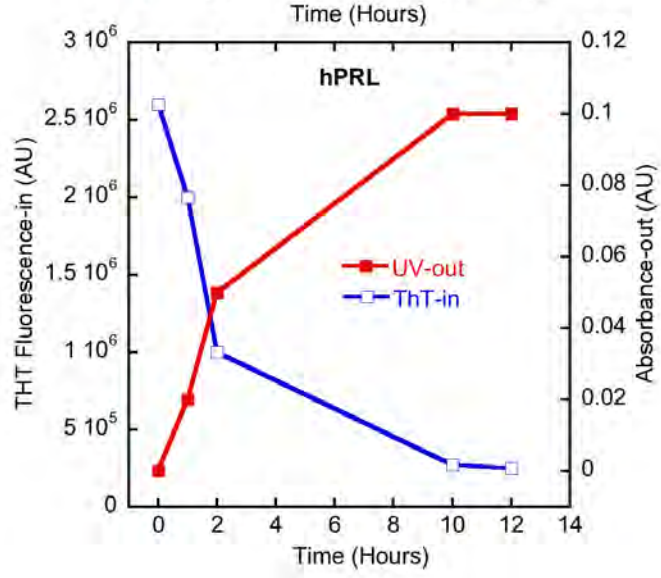
hPRL
UV-out
ThT-in
THT Fluorescence-in (AU)
Absorbance-out (AU)
Time (Hours)
3 10^6
2.5 10^6
2 10^6
1.5 10^6
1 10^6
5 10^5
0
0.12
0.1
0.08
0.06
0.04
0.02
0
0
2
4
6
8
10
12
14

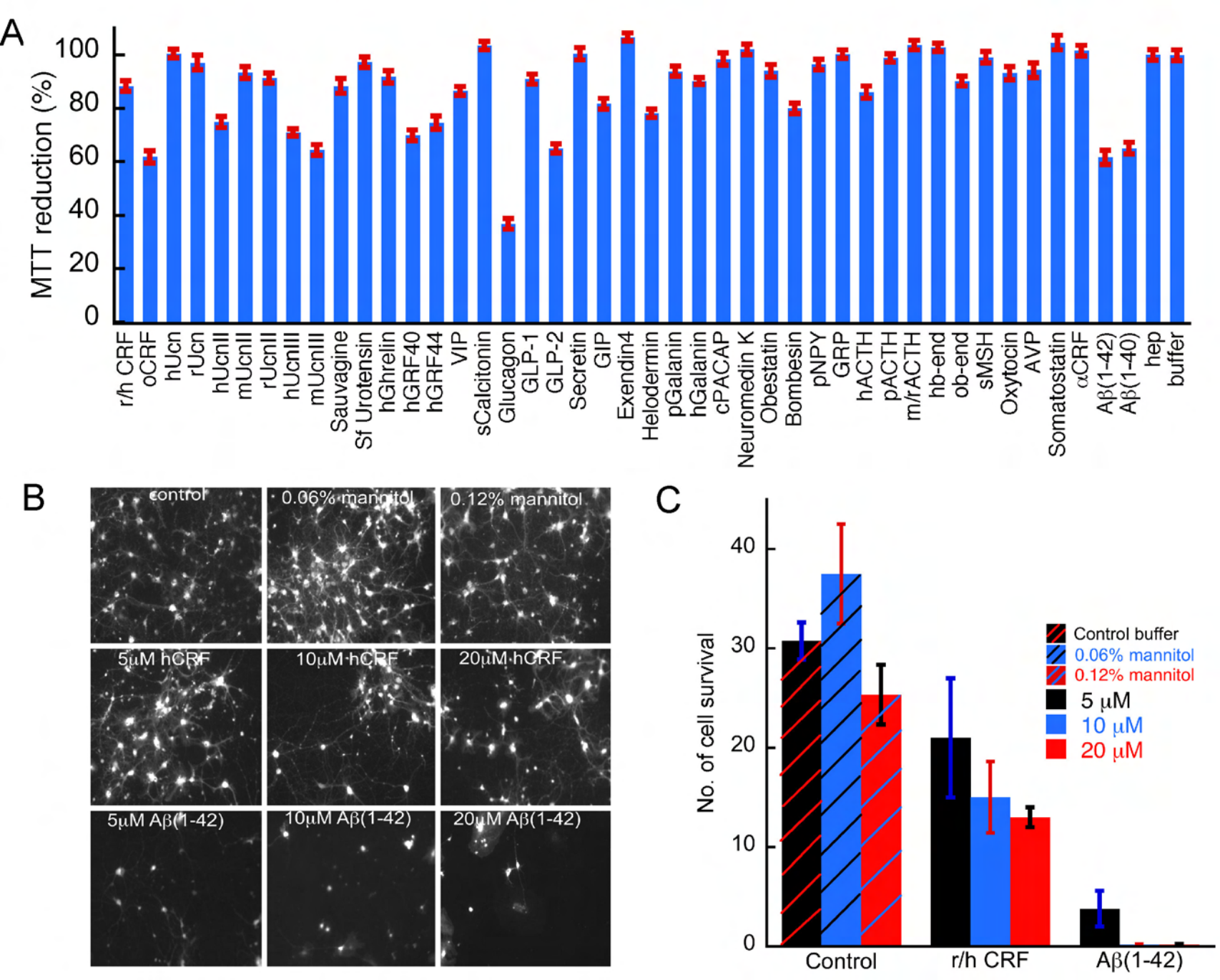
A
MTT reduction (%)
100
80
60
40
20
0
r/h CRF
oCRF
hUcn
rUcn
hUcnII
mUcnII
rUcnII
hUcnIII
mUcnIII
Sauvagine
Sf Urotensin
hGhrelin
hGRF40
hGRF44
VIP
sCalcitonin
Glucagon
GLP-1
GLP-2
Secretin
GIP
Exendin4
Helodermin
pGalanin
hGalanin
cPACAP
Neuromedin K
Obestatin
Bombesin
pNPY
GRP
hACTH
pACTH
m/rACTH
hb-end
ob-end
sMSH
Oxytocin
AVP
Somatostatin
αCRF
Aβ(1-42)
Aβ(1-40)
hep
buffer
B
control
0.06% mannitol
0.12% mannitol
5μM hCRF
10μM hCRF
20μM hCRF
5μM Aβ(1-42)
10μM Aβ(1-42)
20μM Aβ(1-42)
C
No. of cell survival
40
30
20
10
0
Control buffer
0.06% mannitol
0.12% mannitol
5 μM
10 μM
20 μM
Control
r/h CRF
Aβ(1-42)

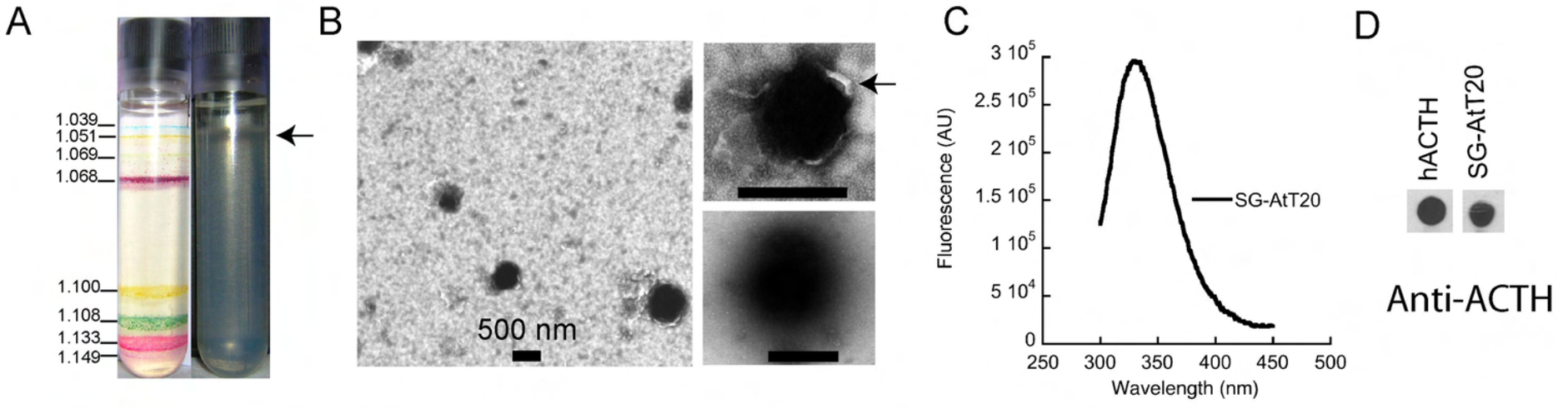
A
1.039
1.051
1.069
1.068
1.100
1.108
1.133
1.149
B
500 nm
C
Fluorescence (AU)
3 10^5
2.5 10^5
2 10^5
1.5 10^5
1 10^5
5 10^4
0
250
300
350
400
450
500
Wavelength (nm)
SG-AtT20
D
hACTH
SG-AtT20
Anti-ACTH

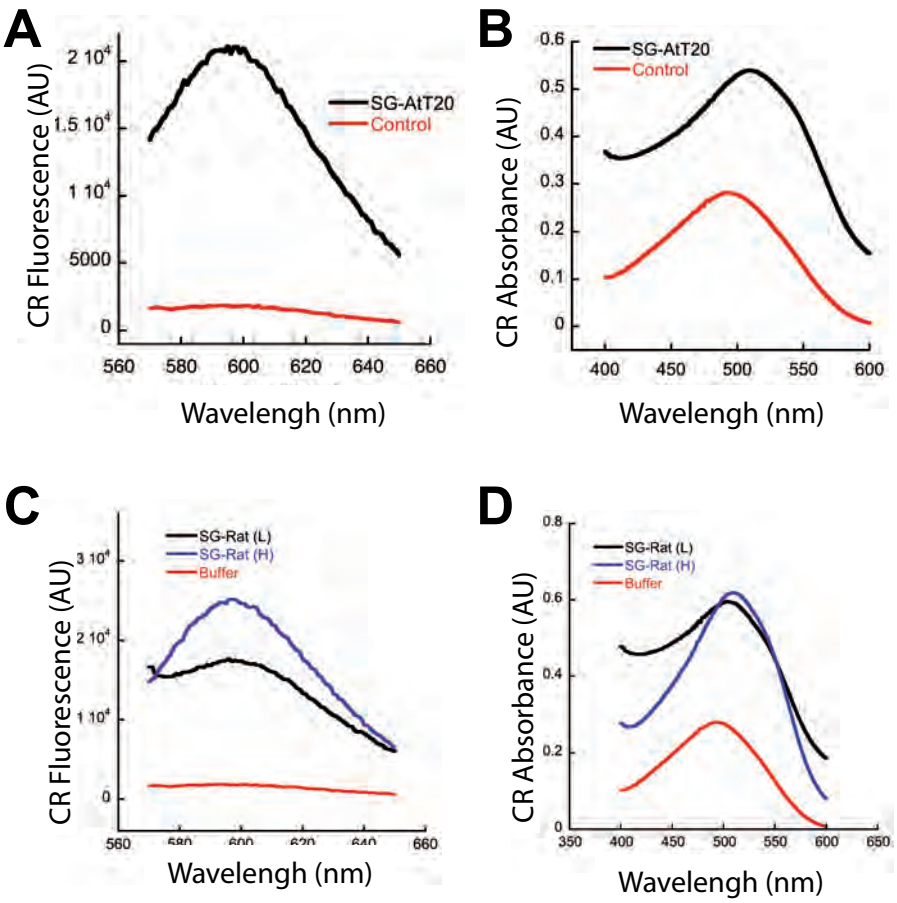
A
CR Fluorescence (AU)
2 10⁴
1.5 10⁴
1 10⁴
5000
0
560
580
600
620
640
660
SG-AtT20
Control
Wavelengh (nm)
B
CR Absorbance (AU)
0.6
0.5
0.4
0.3
0.2
0.1
0
400
450
500
550
600
SG-AtT20
Control
Wavelengh (nm)
C
CR Fluorescence (AU)
3 10⁴
2 10⁴
1 10⁴
0
560
660
SG-Rat (L)
SG-Rat (H)
Buffer
Wavelengh (nm)
D
CR Absorbance (AU)
0.8
0.6
0.4
0.2
0
350
400
450
500
550
600
650
SG-Rat (L)
SG-Rat (H)
Buffer
Wavelengh (nm)

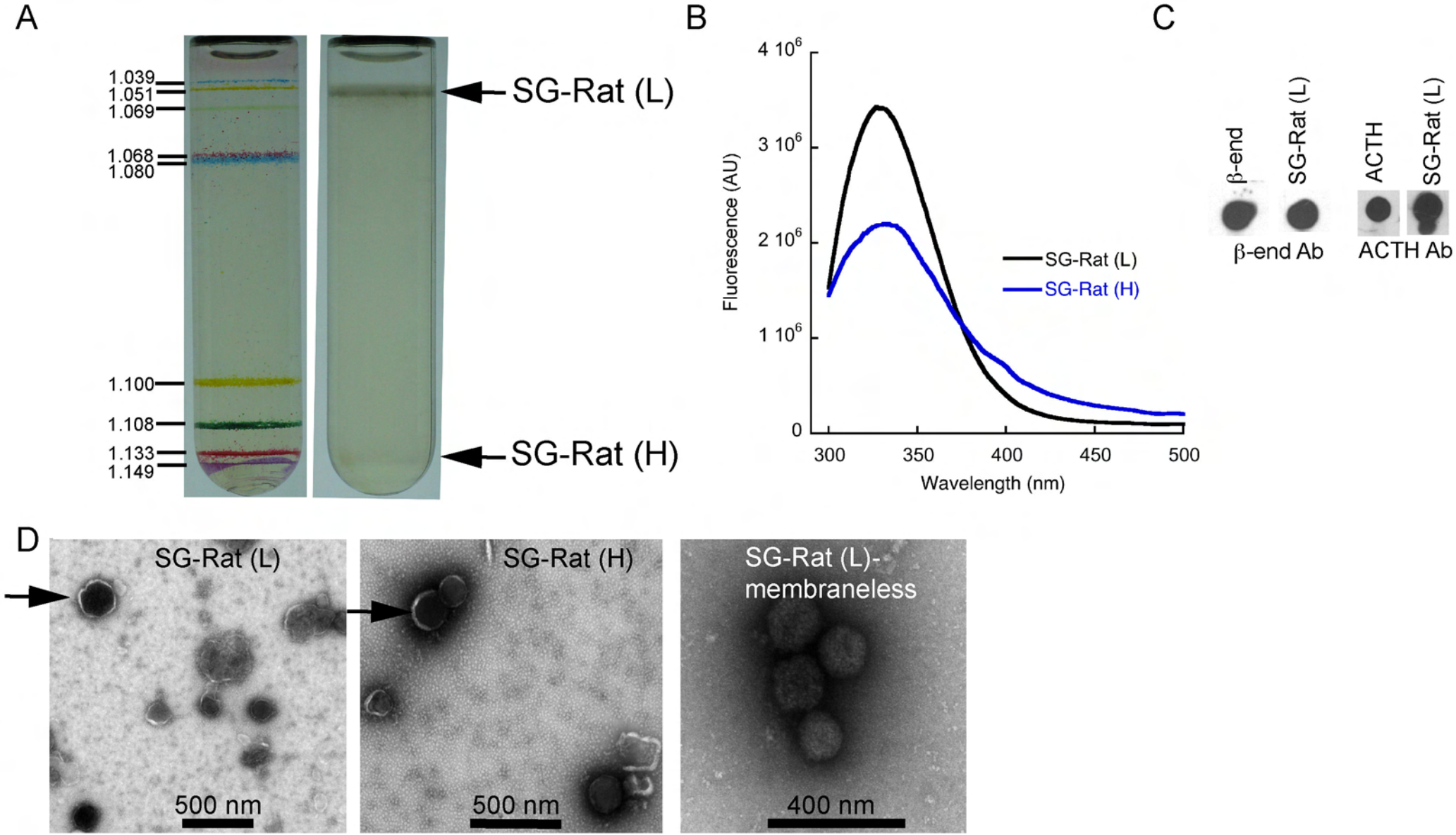
A
1.039
1.051
1.069
1.068
1.080
1.100
1.108
1.133
1.149
SG-Rat (L)
SG-Rat (H)
B
4 10^6
3 10^6
2 10^6
1 10^6
0
Fluorescence (AU)
300
350
400
450
500
Wavelength (nm)
SG-Rat (L)
SG-Rat (H)
C
β-end
SG-Rat (L)
ACTH
SG-Rat (L)
β-end Ab
ACTH Ab
D
SG-Rat (L)
500 nm
SG-Rat (H)
500 nm
SG-Rat (L)-
membraneless
400 nm

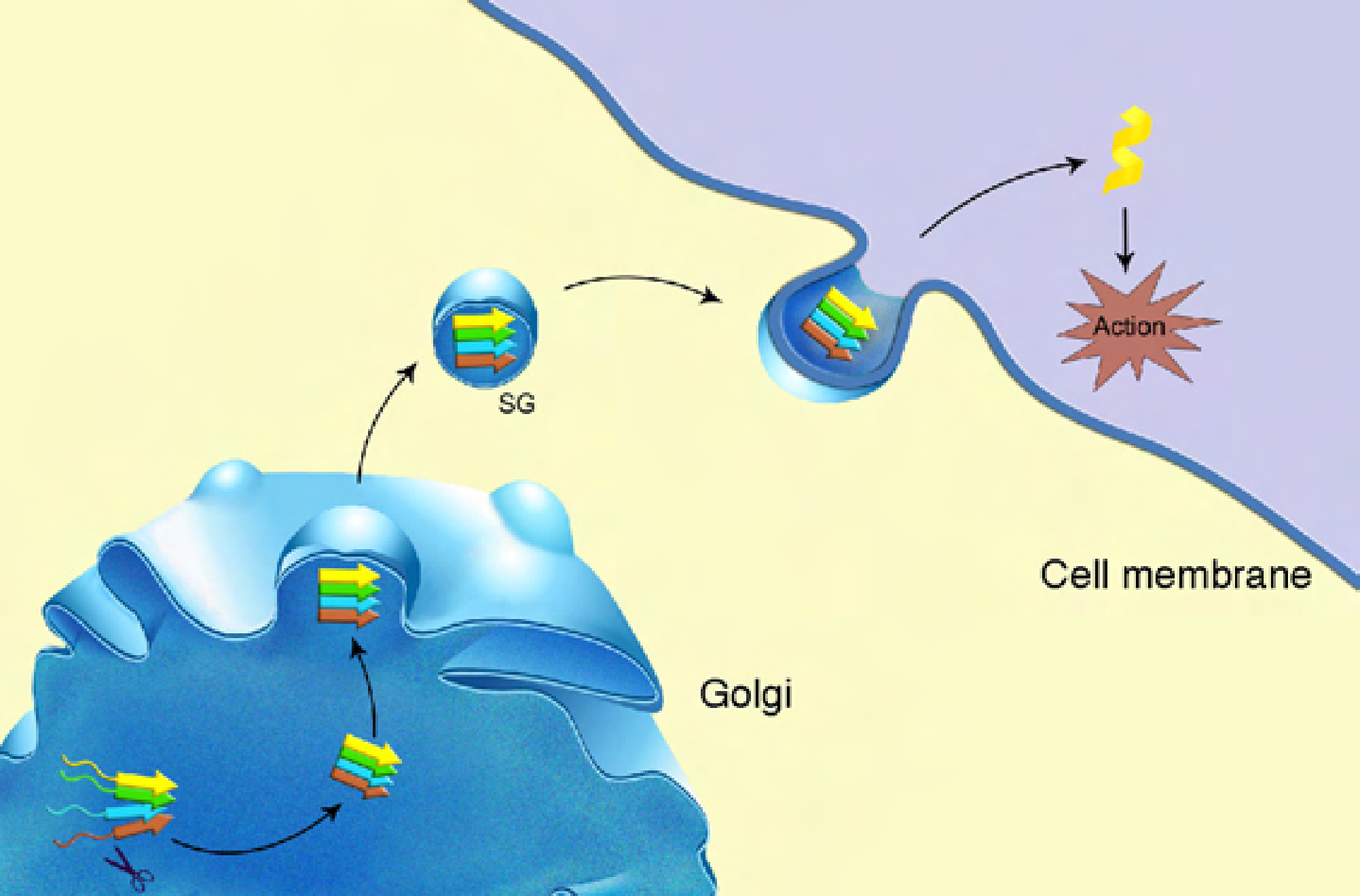
SG
Action
Cell membrane
Golgi